Annals of Biomedical Engineering, Vol. 38, No. 4, April 2010 (© 2010) pp. 1683–1701
DOI: 10.1007/s10439-010-9948-y

Erratum

Erratum to: Blood HbO_2 and $HbCO_2$ Dissociation Curves at Varied O_2, CO_2, pH, 2,3-DPG and Temperature Levels

RANJAN K. DASH and JAMES B. BASSINGTHWAIGHTE

Department of Bioengineering, University of Washington, Box 355061, N210G North Foege Bldg, 1705 NE Pacific St., Seattle, WA 98195-5061, USA

Abstract—New mathematical model equations for O_2 and CO_2 saturations of hemoglobin (S_{HbO_2} and S_{HbCO_2}) are developed here from the equilibrium binding of O_2 and CO_2 with hemoglobin inside RBCs. They are in the form of an invertible Hill-type equation with the apparent Hill coefficients K_{HbO_2} and K_{HbCO_2} in the expressions for S_{HbO_2} and S_{HbCO_2} dependent on the levels of O_2 and CO_2 partial pressures (P_{O_2} and P_{CO_2}), pH, 2,3-DPG concentration, and temperature in blood. The invertibility of these new equations allows P_{O_2} and P_{CO_2} to be computed efficiently from S_{HbO_2} and S_{HbCO_2} and vice versa. The oxyhemoglobin (HbO_2) and carbamino-hemoglobin ($HbCO_2$) dissociation curves computed from these equations are in good agreement with the published experimental and theoretical curves in the literature. The model solutions describe that, at standard physiological conditions, the hemoglobin is about 97.2% saturated by O_2 and the amino group of hemoglobin is about 13.1% saturated by CO_2. The O_2 and CO_2 content in whole blood are also calculated here from the gas solubilities, hematocrits, and the new formulas for S_{HbO_2} and S_{HbCO_2}. Because of the mathematical simplicity and invertibility, these new formulas can be conveniently used in the modeling of simultaneous transport and exchange of O_2 and CO_2 in the alveoli–blood and blood–tissue exchange systems.

Keywords—Mathematical modeling, Hill equation, Oxyhemoglobin and carbamino-hemoglobin dissociation curves, Effects of pH, 2,3-diphosphoglycerate, and temperature, Nonlinear O_2–CO_2 interactions, Bohr and Haldane effects.

Address correspondence to James B. Bassingthwaighte, Department of Bioengineering, University of Washington, Box 355061, N210G North Foege Bldg, 1705 NE Pacific St., Seattle, WA 98195-5061, USA. Electronic mail: jbb2@washington.edu

History: This article corrects the errors made in the publication of the original article (Dash RK and Bassingthwaighte JB. Blood HbO_2 and $HbCO_2$ dissociation curves at varied O_2, CO_2, pH, 2,3-DPG and temperature levels. Ann Biomed Eng 32(12):1676-1693, 2004.) when the publisher failed to send galley proofs to the authors for review. Corrections were listed as an appendix to a later publication (Dash RK and Bassingthwaighte JB. Simultaneous blood–tissue exchange of oxygen, carbon dioxide, bicarbonate and hydrogen ion. Ann Biomed Eng 34(7): 1129–1148. 2006), except for one in Eq. 11 where it should have been specified that the DPG (bisphosphoglycerate) concentration was 4.65 mM, not molar. The equations here match the model code downloadable at www.physiome.org/model/.

The online version of the original article can be found under doi:10.1007/s10439-004-7821-6.

INTRODUCTION

As blood passes through capillaries, the affinity of hemoglobin (Hb) for O_2 and CO_2 changes along the length of the capillary. Each O_2 and CO_2 reduce the affinity of Hb for the other. Changes in pH and temperature have synergistic effects. In metabolizing tissue, the blood warms, becomes more acidic, and carries more CO_2 as it progresses along the capillary; the rising temperature, the diminishing pH, and the rising P_{CO_2} all reduce the affinity of Hb for O_2 and foster O_2 release from Hb into the tissue. The loss of O_2 from Hb into the tissue fosters the uptake of CO_2 by Hb, though this effect is small compared to the buffering by bicarbonate. In the lungs, the reduction in temperature, the loss of CO_2, and the concordant rising of pH all foster increasing the affinity of Hb for O_2. Thus the local influences in lung versus tissue capillaries are ideally suited to maximize the delivery of O_2 from alveolar air to tissues and the removal of CO_2 from tissue to alveolar air. The other solute having a significant influence on the binding of O_2 to Hb is 2,3-diphosphoglycerate (2,3-DPG); raising [2,3-DPG] levels, as occurs with altitude and in diabetes, reduces the O_2 binding to Hb, shifting the oxyhemoglobin (HbO_2) dissociation curve to higher P_{50}s, just like higher CO_2, lower pH and higher temperature do.

Early Development of Oxyhemoglobin Dissociation Descriptions

Numerous mathematical models have been proposed in the literature to describe the standard and nonstandard HbO_2 "equilibrium" dissociation curves

since the pioneering work of Hill[13] and Adair.[1] These are reviewed extensively by Roughton,[29] Antonini and Brunori,[2] Baumann *et al.*,[5] and Popel.[27] We shall henceforth, for brevity, call the HbO_2 "equilibrium" dissociation curves the HbO_2 dissociation curves (ODC). Hill[13] originally postulated an *n*th-order one-step kinetic hypothesis for O_2 binding to Hb to derive the simplest model for standard ODC involving only two parameters. Hill's equation for the ODC describes the oxygen saturation S_{O_2} as a function of oxygen partial pressure P_{O_2} relative to the half-saturation level P_{50}:

$$S_{O_2} = \frac{K_{O_2} P_{O_2}^n}{1 + K_{O_2} P_{O_2}^n} = \frac{(P_{O_2}/P_{50})^n}{1 + (P_{O_2}/P_{50})^n} \qquad (1)$$

where K_{O_2} is the Hill coefficient and n is the Hill exponent. They are related by $K_{O_2} = (P_{50})^{-n}$ where P_{50} is the level of P_{O_2} at which Hb is 50% saturated by O_2. The value $n = 2.7$ was found to fit well to the data for normal human blood in the saturation range of 20–98%[29] for which the value of P_{50} is about 26.8 mmHg. This gives $K_{O_2} = 1.3933 \times 10^{-4}$ mmHg^{-n}. Hill's equation is analytically invertible.

Subsequently, Adair[1] postulated a more realistic four-step kinetic hypothesis (known as the intermediate compound hypothesis) and derived a more accurate formula for standard ODC involving four distinct parameters. Because of its better accuracy, Adair's equation has been particularly useful in the analysis of experimental data at very low and very high P_{O_2}'s.[28,30,40] Winslow *et al.*[39] developed an algorithm for computing the nonstandard ODCs by analyzing fresh human whole blood data over a range of O_2 and CO_2 partial pressures, pH, and [DPG]/[Hb] concentration ratio using the Adair's equation. O'Riordan *et al.*[26] compared nine different models, including Hill's equation and Adair's equation, by fitting them to the data for normal human whole blood. Hill's equation was found to give good characterization of the data over the saturation range of 20–98%, confirming the earlier finding of Roughton,[29] which is the range of major physiological interest. However, Adair's equation was found to be accurate at saturations approaching 100% and was good also down to a little less than 10% saturation (see also Baumann *et al.*,[5] Roughton,[28] Roughton *et al.*,[29] Roughton and Severinghaus[30]).

The Need for a Model with Practical Accuracy and Convenience

The aim of this study is to provide an expression describing the relationship between hemoglobin saturation and P_{O_2} over a wide range of not only P_{O_2} but P_{CO_2}, pH, 2,3-DPG, and temperature, a total of five variables. It is furthermore important that this expression be invertible so that one can convert from observations on a blood sample to the relevant chemical driving forces and to the total contents of oxygen and carbon dioxide in the blood. Our efforts in searching for extensive data sets covering large ranges of these five variables met with failure: Winslow *et al.*'s[40] data were by far the most extensive, but the original data tables have not been preserved, though of course they are summarized by the P_{50}'s he reported. Consequently we have been reduced to fitting these "summaries" defined through other models rather than performing optimizations to parameterize our new, more broadly defined model against original experimental observations. This compromise is acceptable because of the many observations and analyses (referenced above and in the following paragraphs) on which it is based.

Development of Further Oxyhemoglobin Models

Margaria *et al.*[25] and Margaria[24] modified Adair's equation by expressing the four Adair constants in terms of two distinct parameters, one representing the O_2 affinity for first three heme sites and the other representing an increased affinity for fourth oxygenation. Subsequently, Kelman[18] proposed an empirical formula (also see Kelman[19]) for converting O_2 tension into its saturation; it is a little more complicated than Adair's, using seven distinct parameters. For nonstandard physiological conditions, a virtual O_2 tension was computed as a function of pH, P_{CO_2}, and temperature from the experimental data and curve-fitting results of Severinghaus.[32] Kelman's formula gives negative values of S_{O_2} for $P_{O_2} < 10$ mmHg, the physically unrealistic values indicating failure of the algorithm in the region 0 mmHg $< P_{O_2} <$ 10 mmHg. Later, Kelman[20] proposed a quadratic formula for S_{O_2} for this range. It is worth pointing out here that the models proposed by Adair,[1] Margaria,[24] and Kelman[18] are not analytically invertible. Therefore, to obtain P_{O_2} from S_{O_2}, an iterative numerical method had to be employed.

Severinghaus[33] developed a simple and accurate empirical formula for standard ODC by modifying Hill's equation. For nonstandard physiological conditions, appropriate P_{O_2} factors for pH, base excess and temperature were used, assuming as usual that these variations do not alter the shape of the curve. The significance of this model is that it fits the normal human blood data to within ± 0.0055 S_{O_2} in the range $0 < S_{O_2} < 1$. Later, Ellis[9] and Severinghaus[34] established that Severinghaus's[33] model is analytically invertible. The motivation behind Severinghaus's[33] new model is that Roughton was never satisfied with the Adair's equation as he could not use the normal

human blood data to generate the needed unique set of Adair's constants and get a good O_2 saturation curve (e.g., see Roughton *et al.*[28,30] and Roughton and Severinghaus[30]). Adair's equation does not accommodate the Hb affinity change for O_2 which occurs when the second O_2 is bound to Hb and the shape of the Hb molecule changes. Severinghaus's[33] new cubic formula accounts for this affinity change and fits the data far better. Later, Siggaard-Andersen *et al.*[37] developed a different empirical formula for standard and nonstandard ODCs which fits very well to the model and data of Severinghaus.[33] However, Siggaard-Andersen *et al.*'s[37] equation is not analytically invertible and requires an iterative numerical method for inversion (e.g., they used a Newton–Raphson method).

Easton[8] proposed a new paradigm involving two parameters for characterizing the standard ODC. His mathematical description was based on the assumption that the formation of HbO_2, and hence O_2 saturation of Hb, is exponentially related to the O_2 partial pressure. Buerk[6] modified Easton's formula and fitted it to normal human and dog blood data[30,33,40] using a linear regression algorithm; the modified Easton's model was found to fit well to the data in the saturation range of 0 to 95%, providing the same accuracy as that of Adair's model. Buerk and Bridges[7] further modified Easton's formula and developed an algorithm for computing the nonstandard ODCs with varying pH, CO_2 partial pressure, [DPG]/[Hb] concentration ratio, and temperature. The dissociation curves computed through this revised formula were found to agree well with those computed from the algorithms of Kelman[18,19] and Winslow *et al.*[39] The model proposed by Easton[8] and subsequently modified by Buerk[6] and Buerk and Bridges[7] is analytically invertible, so one can efficiently calculate S_{O_2} from P_{O_2} and vice versa. However, since these models are good only up to 95% S_{O_2}, we have developed the present model which is good above this level.

Carboxyhemoglobin

There are few mathematical models available in the literature for computing the CO_2 saturation of hemoglobin and CO_2 content in whole blood. Kelman[21] described an algorithm for computing the whole blood CO_2 content from the levels of pH, CO_2 tension, O_2 saturation and temperature in blood. Forster *et al.*[10] and Forster[11] have studied the rate of reaction of CO_2 with Hb to form $HbCO_2$ (carbamino-hemoglobin) at various physiological conditions. Hill *et al.*[14–16] and Salathe *et al.*[31] have computed the concentration of $HbCO_2$ during O_2 and CO_2 exchange through mathematical modeling by accounting for the physical and biochemical processes including the acid–base balance. Later, Singh *et al.*,[38] extending their earlier work,[36] developed mathematical formulas for nonstandard HbO_2 and $HbCO_2$ dissociation curves from the equilibrium binding of O_2 and CO_2 with Hb inside RBCs; these were similar to Hill's equation but included the effects of P_{O_2}, P_{CO_2} and pH. However, the effects of 2,3-DPG and temperature were not established. More recently, Huang and Hellums[17] developed a computational model for convective-diffusive gas (O_2 and CO_2) transport in the microcirculation and in oxygenators by accounting for the acid–base regulation and the Bohr and Haldane effects (increasing P_{CO_2} or pH reduces O_2 affinity of Hb and increasing P_{O_2} reduces CO_2 affinity of Hb).

The Consequence of This Study

This study fulfills an important requirement in the physiological studies of simultaneous O_2 and CO_2 transport and exchange by including the influences of Hb-mediated nonlinear O_2–CO_2 interactions[14–17,31] and the related changes in pH that occur with passage through capillaries in tissues and in the lung. Accounting for both Bohr and Haldane effects is crucial in the modeling of simultaneous transport and exchange of O_2 and CO_2 in the circulatory system. For example, an important clinical application using the results of the present work is in using ^{15}O-oxygen positron emission tomography (PET) and in the analysis of signals from BOLD (blood oxygen level dependent) MRI (magnetic resonance imaging). Our governing equations account for O_2 saturation of Hb as well as CO_2 saturation of Hb, which are coupled or linked to each other through the kinetics of O_2 and CO_2 binding to Hb. With this motivation, by considering a detailed mathematical analysis of the equilibrium binding of O_2 and CO_2 with Hb inside RBCs, including the nonlinear O_2–CO_2 interactions and the effects of pH, 2,3-DPG and temperature, we end up with relatively simple model equations for nonstandard HbO_2 and $HbCO_2$ dissociation curves, as well as the O_2 and CO_2 contents in whole blood.

The equations for O_2 and CO_2 saturations of Hb (S_{HbO_2} and S_{HbCO_2}) are of the form of a Hill-type equation which is invertible. The apparent Hill coefficients K_{HbO_2} and K_{HbCO_2} in the expression for S_{HbO_2} and S_{HbCO_2} are explicitly dependent on the levels of O_2 and CO_2 partial pressures, pH, 2,3-DPG concentration, and temperature in blood. The results show that, at normal physiological conditions, Hb is about 97.2% saturated by O_2 and the amino group of Hb is about 13.1% saturated by CO_2. The invertibility of our model equations for S_{HbO_2} and S_{HbCO_2} allows their convenient usage in computationally complex models of simultaneous transport and exchange of O_2 and

CO_2 in the pulmonary and systemic circulations. The mathematical modeling language (MML) code for our model, which is implemented in our Java Simulation (JSim) interface, is available for download and public use at http://physiome.org/Models/GasTransport/.

MATHEMATICAL FORMULATION

Governing Biochemical Reactions

The dynamics of hemoglobin-facilitated transport of O_2 and CO_2 in blood and their nonlinear interactions are governed by the following biochemical reactions inside RBCs.[2,14,29,31,38] Hemoglobin, Hb, consists of four heme-amino chains, two α and two β chains; each contains a heme group, Hm, which binds to an O_2 molecule and has a terminal amino group, $-NH_2$, which can bind to a CO_2 molecule to form an ionizable carbamino terminus, –NHCOOH. We consider the α and β chains to be identical in their binding with CO_2. The four heme sites for O_2 binding show cooperativity so that an HbO_2 saturation curve has a Hill exponent of about 2.7. Therefore, we consider Hb as of 4 Hm (i.e., Hb = Hm_4). The governing reactions are:

CO_2 hydration reaction—HCO_3^-, buffering of CO_2:

$$CO_2 + H_2O \underset{kb_1'}{\overset{kf_1'}{\leftrightarrows}} H_2CO_3 \overset{K_1''}{\leftrightarrows} HCO_3^- + H^+ \tag{2a}$$

CO_2 binding to $HmNH_2$ chains—$HmNHCOO^-$ buffering of CO_2:

$$CO_2 + HmNH_2 \underset{kb_2'}{\overset{kf_2'}{\leftrightarrows}} HmNHCOOH \overset{K_2''}{\leftrightarrows} HmNHCOO^- + H^+. \tag{2b}$$

CO_2 binding to O_2HmNH_2 chains—$O_2HmNHCOO^-$ buffering of CO_2:

$$CO_2 + O_2HmNH_2 \underset{kb_3'}{\overset{kf_3'}{\leftrightarrows}} O_2HmNHCOOH \overset{K_3''}{\leftrightarrows} O_2HmNHCOO^- + H^+. \tag{2c}$$

O_2 binding to $HmNH_2$ chains—one-step kinetics using the P_{O_2}-dependent values of the rates of association and dissociation to accounts for the cooperativity.

$$O_2 + HmNH_2 \underset{kb_4'}{\overset{kf_4'}{\leftrightarrows}} O_2HmNH_2. \tag{2d}$$

Ionization of $HmNH_2$ chains—pH buffering:

$$HmNH_3^+ \overset{K_5''}{\leftrightarrows} HmNH_2 + H^+. \tag{2e}$$

Ionization of O_2HmNH_2 chains—pH buffering:

$$O_2HmNH_3^+ \overset{K_6''}{\leftrightarrows} O_2HmNH_2 + H^+. \tag{2f}$$

$HmNH_2$ and O_2HmNH_2 refer to the reduced and oxygenated heme sites attached to the amino chain, $HmNH_3^+$ and $O_2HmNH_3^+$ denote their ionized forms; HmNHCOOH and O_2HmNHCOOH refer to the reduced and oxygenated carbamino chain, $HmNHCOO^-$ and $O_2HmNHCOO^-$ denote their ionized forms; kf_i' and kb_i' are the rate constants of forward and backward direction reactions; K_1'', K_2'', K_3'', K_5'' and K_6'' are the ionization constants of H_2CO_3, HmNHCOOH, O_2HmNHCOOH, $HmNH_3^+$ and $O_2HmNH_3^+$. The units of kf_1', kf_2', kf_3', and kf_4' are $M^{-1}\,s^{-1}$; kb_1', kb_2', kb_3', and kb_4' are in s^{-1}; K_1'', K_2'', K_3'', K_5'' and K_6'' are in M.

In plasma, the CO_2 hydration reaction (2a) is slow, but it is fast within RBCs because there is carbonic anhydrase in the cytosol and on the membrane. The uptake of O_2 and CO_2 by Hb inside RBCs is governed by reactions (2b), (2c) and (2d). Reactions (2e) and (2f) act as a buffer system and control the concentration of H^+ in RBCs. The interaction between O_2 and CO_2 is mediated by the proton H^+ within RBCs via reactions (2a) to (2f).

The binding of CO_2 with the four amino groups of a hemoglobin molecule is noncooperative in nature. So the kinetics of CO_2 uptake by Hb can be represented by reactions (2b) and (2c) with the rate and equilibrium constants fixed. However, the binding of O_2 with Hb takes place in four intermediate steps and is cooperative in nature due to the interactions between the binding heme sites.[2] To account for this through our one-step kinetic approach in reaction (2d), we use the equilibrium "constant" $K_4'(= kf_4'/kb_4')$ a function of O_2 partial pressure P_{O_2}; K_4' also depends on the levels of pH, P_{CO_2}, 2,3-DPG concentration, and temperature inside the RBCs.[4]

Equilibrium Relations

The reactions (2a)–(2f) are not instantaneous and can be described through a set of ordinary differential equations. However, these reactions approach equilibrium within about 20 ms, so the equilibrium descriptions through algebraic equations are very close to the truth. Therefore, from here on, we use the ratios

of the on-to-off rate constants, that is, the equilibrium constants, instead of the rate constants. At equilibrium, we obtain the following set of algebraic relations from the set of reactions (2a)–(2f), where we denote [·] as the concentration of a species in the water space of RBCs:

$$K_1'[CO_2] = [H_2CO_3], \tag{3a}$$

$$K_1''[H_2CO_3] = \left[HCO_3^-\right][H^+], \tag{3b}$$

$$K_2'[CO_2][HmNH_2] = [HmNHCOOH], \tag{3c}$$

$$K_2''[HmNHCOOH] = [HmNHCOO^-][H^+], \tag{3d}$$

$$K_3'[CO_2][O_2HmNH_2] = [O_2HmNHCOOH], \tag{3e}$$

$$K_3''[O_2HmNHCOOH] = [O_2HmNHCOO^-][H^+], \tag{3f}$$

$$K_4'[O_2][HmNH_2] = [O_2HmNH_2], \tag{3g}$$

$$K_5''\left[HmNH_3^+\right] = [HmNH_2][H^+], \tag{3h}$$

$$K_6''\left[O_2HmNH_3^+\right] = [O_2HmNH_2][H^+], \tag{3i}$$

where the equilibrium constants K_1', K_2', K_3', and K_4' are defined by

$$K_1' = \frac{kf_1'}{kb_1'}[H_2O], \quad K_2' = \frac{kf_2'}{kb_2'}, \quad K_3' = \frac{kf_3'}{kb_3'}, \quad K_4' = \frac{kf_4'}{kb_4'}. \tag{4}$$

Pure water (H_2O) has a molecular weight of 18 g/mole so that its concentration in plasma, which is 94% water, is about $55.56 \times 0.94 = 52.23$ M which is very high as compared to the total solute concentration (280 mM) in plasma. This leads to K_1' being practically a constant. The units of K_2', K_3' and K_4' are M^{-1}; K_1' is unitless; K_4' is dependent on $[O_2]$, $[CO_2]$, $[H^+]$, [2,3-DPG] and T.

The concentrations of total hemoglobin, total O_2-bound hemoglobin, and total CO_2-bound hemoglobin in RBCs are given by

$$\begin{aligned}[Hb] = 4([HmNH_2] &+ \left[HmNH_3^+\right] + [HmNHCOOH] \\ &+ [HmNHCOO^-] + [O_2HmNH_2] \\ &+ \left[O_2HmNH_3^+\right] + [O_2HmNHCOOH] \\ &+ [O_2HmNHCOO^-]),\end{aligned} \tag{5a}$$

$$\begin{aligned}[HbO_2] = 4([O_2HmNH_2] &+ \left[O_2HmNH_3^+\right] \\ &+ [O_2HmNHCOOH] \\ &+ [O_2HmNHCOO^-]),\end{aligned} \tag{5b}$$

$$\begin{aligned}[HbCO_2] = 4([HmNHCOOH] &+ [HmNHCOO^-] \\ &+ [O_2HmNHCOOH] \\ &+ [O_2HmNHCOO^-]).\end{aligned} \tag{5c}$$

The values of –NHCOOH dissociation constants K_2'' and K_3'' are usually higher than 10^{-6} M[10,11] while the concentration of H^+ in RBCs is about 5.75×10^{-8} M (i.e., pH in RBCs is about 7.24 when pH in plasma is about 7.4). So the concentrations of HmNHCOOH and O_2HmNHCOOH are usually two orders of magnitude smaller than those of HmNHCOO$^-$ and O_2HmNHCOO$^-$.[14] Nevertheless, extending the work of Singh *et al.*,[38] we include the contributions of HmNHCOOH and O_2HmNHCOOH for conceptual completeness and improved accuracy.

Using Eqs. (3c)–(3i) in Eqs. (5a), (5b) and (5c), we obtain the following explicit expressions for the concentrations of total hemoglobin, total O_2-bound hemoglobin, and total CO_2-bound hemoglobin in RBCs:

$$\begin{aligned}[Hb] = 4[HmNH_2] &\times \left[\left(K_2'[CO_2]\left\{1 + \frac{K_2''}{[H^+]}\right\} + \left\{1 + \frac{[H^+]}{K_5''}\right\}\right)\right. \\ &+ K_4'[O_2]\left(K_3'[CO_2]\left\{1 + \frac{K_3''}{[H^+]}\right\}\right. \\ &\left.\left. + \left\{1 + \frac{[H^+]}{K_6''}\right\}\right)\right],\end{aligned} \tag{6a}$$

$$\begin{aligned}[HbO_2] = 4[HmNH_2]&\left[K_4'[O_2]\left(K_3'[CO_2]\left\{1 + \frac{K_3''}{[H^+]}\right\}\right.\right. \\ &\left.\left. + \left\{1 + \frac{[H^+]}{K_6''}\right\}\right)\right],\end{aligned} \tag{6b}$$

$$\begin{aligned}[HbCO_2] = 4[HmNH_2]&\left[\left(K_2'[CO_2]\left\{1 + \frac{K_2''}{[H^+]}\right\}\right)\right. \\ &\left. + K_4'[O_2]\left(K_3'[CO_2]\left\{1 + \frac{K_3''}{[H^+]}\right\}\right)\right].\end{aligned} \tag{6c}$$

Expressions for S_{HbO_2} and S_{HbCO_2}

The fractional O_2 and CO_2 saturations of Hb (S_{HbO_2} and S_{HbCO_2}) is obtained from Eqs. (6a), (6b) and (6c) as the ratios $[HbO_2]/[Hb]$ and $[HbCO_2]/[Hb]$. Putting these in the form of the Hill[13] equation gives the advantage of their being analytically invertible, allowing the O_2 and CO_2 concentrations ($[O_2]$ and $[CO_2]$), or their partial pressures (P_{O_2} and P_{CO_2}), to be

calculated efficiently from their fractional saturations (S_{HbO_2} and S_{HbCO_2}) and vice versa (see Appendix B). These expressions for S_{HbO_2} and S_{HbCO_2} are formulated as for single-site binding and a Hill *exponent* of unity and therefore using concentration-dependent Hill coefficients:

$$S_{HbO_2} = \frac{[HbO_2]}{[Hb]} = \frac{K_{HbO_2}[O_2]}{1 + K_{HbO_2}[O_2]}, \tag{7a}$$

$$S_{HbCO_2} = \frac{[HbCO_2]}{[Hb]} = \frac{K_{HbCO_2}[CO_2]}{1 + K_{HbCO_2}[CO_2]}, \tag{7b}$$

where the apparent Hill coefficients K_{HbO_2} and K_{HbCO_2} (with units M^{-1}) account for the influences of P_{O_2}, P_{CO_2}, pH, [2,3-DPG] and T as well as the nonlinear O_2–CO_2 interactions on the binding of O_2 and CO_2 with Hb inside RBCs. These concentration-dependent Hill coefficients are quite different from the constant-valued Hill coefficient of Eq. (1). The expressions for K_{HbO_2} and K_{HbCO_2} are given by

$$K_{HbO_2} = \frac{K_4'\left(K_3'[CO_2]\left\{1 + \frac{K_3''}{[H^+]}\right\} + \left\{1 + \frac{[H^+]}{K_6''}\right\}\right)}{\left(K_2'[CO_2]\left\{1 + \frac{K_2''}{[H^+]}\right\} + \left\{1 + \frac{[H^+]}{K_5''}\right\}\right)}, \tag{8a}$$

$$K_{HbCO_2} = \frac{\left(K_2'\left\{1 + \frac{K_2''}{[H^+]}\right\}K_3'K_4' + \left\{1 + \frac{K_3''}{[H^+]}\right\}[O_2]\right)}{\left(\left\{1 + \frac{[H^+]}{K_5''}\right\} + K_4'\left\{1 + \frac{[H^+]}{K_6''}\right\}[O_2]\right)}. \tag{8b}$$

K_{HbO_2} and K_{HbCO_2} depend on [2,3-DPG] and T through their dependency on K_4' (see below). The P_{50} for 50% HbO_2 saturation is not a constant, but also a function of P_{CO_2}, pH, [2,3-DPG] and T. Note that the form of Eqs. (7a) and (7b) is first order and that the Hill exponent inferred by analogy to Eq. (1) is unity. This means that the fundamental S-shape of the HbO_2 dissociation curve is built into the dependency of K_{HbO_2} on $[O_2]$. The linkage between K_{HbO_2} and K_{HbCO_2} can be deduced from the fact that the equilibrium constants K_2', K_2'' and K_5'' for deoxygenated Hb are higher than K_3', K_3'' and K_6'' for oxygenated Hb.

Expression for K_4'

The forward rate constant Kf_4' for the association of O_2 with $HmNH_2$ and the backward rate constant Kb_4' for the dissociation of O_2 from O_2HmNH_2 depend on the levels of P_{O_2}, P_{CO_2}, pH, [2,3-DPG] and T in RBCs.[4] We characterize the dependency of the equilibrium constant $K_4' = kf_4'/kb_4'$ on $[O_2]$, $[CO_2]$, $[H^+]$, [2,3-DPG] and T through the following power-law proportionality equation:

$$\begin{aligned} K_4' &= K_4''\left\{\frac{[O_2]}{[O_2]_S}\right\}^{n_0}\left\{\frac{[H^+]}{[H^+]S}\right\}^{-n_1}\left\{\frac{[CO_2]}{[CO_2]_S}\right\}^{-n_2} \\ &\quad \times \left\{\frac{[DPG]}{[DPG]_S}\right\}^{-n_3}\left\{\frac{T}{T_S}\right\}^{-n4} \\ &= K_4''\left\{\frac{[O_2]}{146\ \mu M}\right\}^{n_0}\left\{\frac{[H^+]}{57.5\ nM}\right\}^{-n_1} \\ &\quad \times \left\{\frac{[CO_2]}{1.31\ mM}\right\}^{-n_2}\left\{\frac{[DPG]}{4.65\ mM}\right\}^{-n_3}\left\{\frac{T}{310^\circ\ K}\right\}^{-n4}, \end{aligned} \tag{9}$$

where the proportionality equilibrium constant K_4'' and the empirical exponents n_i, $i = 0, 1, \ldots, 4$, are to be determined. The subscript "S" refers to the values under standard physiological conditions in the arterial system: $[O_2]_S = 146\ \mu M$ (or $P_{O_{2,S}} = 100$ mmHg), $[CO_2]_S = 1.31$ mM (or $P_{CO_{2,S}} = 40$ mmHg), $[H^+]_S = 57.5$ nM (or $pH_S = 7.24$), $[2,3\text{-DPG}]_S = 4.65$ mM, and $T_S = 310$ K = 37 °C in RBCs (see Table 1). At these conditions $K_4' = K_4''$; so K_4'' is also in the units of M^{-1}. The standard hematocrit, *Hct*, is about 0.45 and the Hb concentration in blood, $[Hb]_{bl}$, is about 0.15 g/mL or 2.33 mM taking the molecular weight of Hb to be 64458.[19] Thus, $[Hb]_{rbc}$ is about 5.18 mM. Buerk and Bridges[7] have used the molar concentration ratio [2,3-DPG]/[Hb] as 0.9 which corresponds to [2,3-DPG] = 4.65 mM.

Now we see that Eqs. (8a) and (8b) along with Eq. (9) completely determine the apparent Hill coefficients K_{HbO_2} and K_{HbCO_2}. Singh *et al.*[38] did not account for the effects of $[CO_2]$, [2,3-DPG] and T on the equilibrium constant K_4' in their modeling. So their case corresponds to Eq. (9) with $n_2 = n_3 = n_4 = 0$ and nonzero n_0 and n_1.

Expressions for α_{O_2} and α_{CO_2}

The equations for fractional saturations, S_{HbO_2} and S_{HbCO_2}, and apparent Hill coefficients, K_{HbO_2} and K_{HbCO_2}, can be expressed in terms of O_2 and CO_2 partial pressures, P_{O_2} and P_{CO_2}, by expressing the molar concentrations $[O_2]$ and $[CO_2]$ in water space of RBCs in terms of P_{O_2} and P_{CO_2} using Henry's law: $[O_2] = \alpha_{O_2} P_{O_2}$ and $[CO_2] = \alpha_{CO_2} P_{CO_2}$, where α_{O_2} and α_{CO_2} are the solubilities of O_2 and CO_2 in water. At body temperature ($T = 37$ °C), $\alpha_{O_2} = 1.46 \times 10^{-6}$ M mmHg^{-1} and $\alpha_{CO_2} = 3.27 \times 10^{-5}$ M mmHg^{-1}. The variation of α_{O_2} and α_{CO_2} with temperature (T) can be expressed through the following quadratic curve-fit equations[19,21] based on the experimental data of Hedley-Whyte and Laver[12] on α_{O_2} and Austin *et al.*[3]

TABLE 1. The representative values of the parameters used in the model.

Symbol	Definition	Value	Unit	Equation	Reference
K_1''	Ionization constant of H_2CO_3	5.5×10^{-4}	M	2a, 3b	14–16
K_1'	Equilibrium constant for hydration of CO_2 ($K_1' = [H_2O]\ kf_1'/kb_1'$)	1.35×10^{-3}	Unitless	3a, 4	14–16
K_1	Equilibrium constant for overall CO_2 hydration reaction ($K = K_1'K_1''$)	7.43×10^{-7}	M		*
K_2''	Ionization constant of HmNHCOOH	1×10^{-6}	M	2b, 3d	10,11,14,15
K_2'	Equilibrium constant for uptake of CO_2 by reduced hemoglobin ($K_2' = kf_2'/kb_2' = K_2/K_2''$)	29.5	M^{-1}	3c, 4	*
K_2	Equilibrium constant for overall uptake of CO_2 by reduced hemoglobin ($K_2 = K_2'K_2''$)	2.95×10^{-5}	Unitless		2
K_3''	Ionization constant of O_2HmNHCOOH	1×10^{-6}	M	2c, 3f	10,11,14,15
K_3'	Equilibrium constant for uptake of CO_2 by oxygenated hemoglobin ($K_3' = kf_3'/kb_3' = K_3/k_3''$)	25.1	M^{-1}	3e, 4	*
K_3	Equilibrium constant for overall uptake of CO_2 by oxygenated hemoglobin ($K_3 = K_3'K_3''$)	2.51×10^{-5}	Unitless		2
K_4'	Equilibrium constant for uptake of O_2 by hemoglobin under standard physiological conditions ($K_4' = kf_4'/kb_4' = kf_4''/kb_4'' = K_4''$)	202123	M^{-1}	3g, 4, 9	†
K_4''	Proportionality equilibrium constant for uptake of O_2 by hemoglobin	202123	M^{-1}	9	†
K_5''	Ionization constant of $HmNH_3^+$	2.63×10^{-8}	M	2e, 3h	2
K_6''	Ionization constant of $O_2HmNH_3^+$	1.91×10^{-8}	M	2f, 3i	2
$S_{HbO_{2,S}}$	O_2 saturation of hemoglobin under standard physiological conditions	97.2%	Unitless	7a	†
$S_{HbCO_{2,S}}$	CO_2 saturation of hemoglobin under standard physiological conditions	13.1%	Unitless	7b	†
R_{rbc}	Gibbs–Donnan ratio for electrochemical equilibrium across the RBC membrane	0.69	Unitless		14,16,31,38
$n_{0,S}$	Exponent on $[O_2]/[O_2]_S$ in the expression for K_4' under standard physiological conditions	1.7	Unitless	9, 15	†
$n_{1,S}$	Exponent on $[H^+]_S/[H^+]$ in the expression for K_4' under standard physiological conditions	1.06	Unitless	9, 16a	†
$n_{2,S}$	Exponent on $[CO_2]_S/[CO_2]$ in the expression for K_4' under standard physiological conditions	0.12	Unitless	9, 16b	†
$n_{3,S}$	Exponent on $[DPG]_S/[DPG]$ in the expression for K_4' under standard physiological conditions	0.37	Unitless	9, 16c	†
$n_{4,S}$	Exponent on T_S/T in the expression for K_4' under standard physiological conditions	4.65	Unitless	9, 16d	†
Hct	Hematocrit; volume fraction of blood occupied by RBCs	0.45	mL/mL		14–16,31
$[Hb]_{bl}$	Hemoglobin concentration in whole blood	2.33 or 0.15	mM or g/mL		*
$[Hb]_{rbc}$	Hemoglobin concentration in RBCs ($[Hb]_{rbc} = [Hb]_{bl}$ / Hct)	5.18 or 0.33333	mM or g/mL		*
W_{bl}	Fractional water space of blood at $Hct = 0.45$	0.81	mL/mL		*
W_{pl}	Fractional water space of plasma	0.94	mL/mL		23
W_{rbc}	Fractional water space of RBCs	0.65	mL/mL		23
$\alpha_{O_{2,S}}$	Solubility coefficient of O_2 in water at body temperature ($T = 37$ °C)	1.46×10^{-6}	$M \times mmHg^{-1}$	10a	12,19
$\alpha_{CO_{2,S}}$	Solubility coefficient of CO_2 in water at body temperature ($T = 37$ °C)	3.27×10^{-5}	$M \times mmH^{-1}$	10a	3,21
$P_{50,S}$	The level of P_{O_2} at which the hemoglobin is 50% saturated by O_2 at STP	26.8	mmHg		6,7,18,39,40
$P_{50,S}^{CO_2}$	The level of P_{CO_2} at which the hemoglobin is 50% saturated by CO_2 at STP	265	mmHg		†

* Calculated using the formula in "definition" and data in "value" columns.
† Estimated through the current model as described in the "Results" section.
The standard physiological conditions are: $[O_2]_S = 146\ \mu M$ (or $P_{O_{2,S}} = 100$ mmHg), $[CO_2]_S = 1.31\ \mu M$ (or $P_{CO_{2,S}} = 40$ mmHg), $[H^+]_S = 57.5$ nM (or $pH_S = 7.24$), $[2,3\text{-DPG}]_S = 4.65\ \mu M$, and $T_S = 37$ °C inside the RBCs.

on α_{CO_2}, correcting for the plasma fractional water content, W_{pl}:

$$\alpha_{O_2} = \left[1.37 - 0.0137(T-37) + 0.00058(T-37)^2\right] \times \left[10^{-6}/W_{pl}\right] \quad \text{M/mmHg}, \tag{10a}$$

$$\alpha_{CO_2} = \left[3.07 - 0.057(T-37) + 0.002(T-37)^2\right] \times \left[10^{-5}/W_{pl}\right] \quad \text{M/mmHg}, \tag{10b}$$

where $W_{pl} = 0.94$. The first term for α_{O_2} is $(1.37/0.94) \times 10^{-6}$ or 1.46×10^{-6} M $mmHg^{-1}$ and for α_{CO_2}

is $(3.07/0.94) \times 10^{-5}$ or 3.27×10^{-5} M mmHg^{-1}, as mentioned above. The solubility of O_2 and CO_2 decreases as temperature increases.

The HbO_2 and $HbCO_2$ dissociation curves described by Eqs. (7a)–(7b) and (8a)–(8b) require knowing the equilibrium constants K_2', K_3', K_2'' to K_6'' and the empirical exponents n_0, n_1, n_2, n_3 and n_4. From the saturations, S_{HbO_2} and S_{HbCO_2}, the total O_2 and CO_2 contents in whole blood can be calculated as described in Appendix A.

RESULTS: PARAMETER ESTIMATION

The O_2 and CO_2 saturations of Hb (S_{HbO_2} and S_{HbCO_2}) and their whole blood contents ($[O_2]_{bl}$ and $[CO_2]_{bl}$) depend on the physiological state variables P_{O_2}, P_{CO_2}, pH, *Hct*, $[2,3\text{-DPG}]_{rbc}$ and T, empirical exponents n_0, n_1, n_2, n_3 and n_4, and equilibrium constants K_1' to K_3', K_1'' to K_6'' and R_{rbc}. The literature does not provide consistent values for the equilibrium constants. Singh *et al.*[38] estimated some of them in their theoretical studies of HbO_2 and $HbCO_2$ dissociation curves, but their estimates do not match with the experimental values obtained by Roughton,[29] Forster *et al.*[10] and Forster[11] which are the values generally accepted.[2,14–16,31] Singh *et al.*[38] assumed that the Hb molecule has only one amino chain, $-NH_2$, and is capable of binding to only one CO_2 molecule, but Hb has four $-NH_2$ chains and can bind to four CO_2 molecules. Thus, Singh *et al.*'s estimates are not acceptable for the kinetic reactions (2a)–(2f). In the present study, we choose or calculate the equilibrium constant K_1, K_1', K_1'', K_2, K_2', K_2'', K_3, K_3', K_3'', K_5'', K_6'', and R_{rbc} appropriately from the literature (see Table 1 for references) and then estimate the proportionality equilibrium constant K_4'' and the empirical exponents n_0, n_1, n_2, n_3 and n_4 so as to obtain the appropriate forms and shifts in the HbO_2 dissociation curves with respect to the levels of pH_{rbc}, P_{CO_2}, $[DPG]_{rbc}$ and T in accord with experimental observations and their summaries captured in the models of Kelman[18] and Buerk and Bridges.[7] The generality and comprehensiveness of the calculations might seem disadvantaged by their apparent complexity, but in fact the code for the equations is quite simple algebra and is viewable (and downloadable) within three clicks of http://physiome.org/Models/GasTransport.

Calculation of Equilibrium Constants

We choose the values $K_1 = K_1'K_1'' = 7.43 \times 10^{-7}$ M, $K_1'' = 5.5 \times 10^{-4}$ M; $K_2 = K_2'K_2'' = 2.95 \times 10^{-5}$, $K_2'' = 1 \times 10^{-6}$ M, $K_3 = K_3'K_3'' = 2.51 \times 10^{-5}$, $K_3'' = 1 \times 10^{-6}$ M, $K_5'' = 2.63 \times 10^{-8}$ M, and $K_6'' = 1.91 \times 10^{-8}$ M (see Table 1 for references); K_1 is the equilibrium constant of the overall CO_2 hydration reaction (2a); K_2 and K_3 are the equilibrium constants of the overall reaction of CO_2 with the reduced and oxygenated Hb, reactions (2b) and (2c). These give $K_1' = 1.35 \times 10^{-3}$, $K_2' = 29.5$ M^{-1} and $K_3' = 25.1$ M^{-1}, as shown in Table 1. Thus, the equilibrium constants K_2, K_2' and K_5'' for reduced Hb are higher than K_3, K_3' and K_6'' for oxygenated Hb. This indicates that the reduced Hb has a greater ability to bind to CO_2 than does the oxygenated Hb (e.g., see Figs. 24 and 26 of Roughton,[29] and Fig. 10.11 of Antonini and Brunori.[2] The estimation of the proportionality equilibrium constant K_4'' and the empirical exponents n_0, n_1, n_2, n_3 and n_4 are described below.

Calculation of Oxygen P_{50}

The P_{50} for O_2 (the level of P_{O_2} at which Hb is 50% saturated by O_2) is conventionally used as a measure of O_2 affinity of Hb and shift in the HbO_2 dissociation curve (ODC). We first calculate the P_{50} values for nonstandard ODCs as a function of pH_{rbc}, P_{CO_2}, $[DPG]_{rbc}$ and T from the model of Buerk and Bridges[7] which agree well with those obtained experimentally by Winslow *et al.*[39] We then employ the method of regression analysis to determine the curve-fit polynomials for these computed P_{50} values recursively with one of the variables varying and the other three fixed at their standard physiological values. We found that the $P_{50}(pH_{rbc})$, $P_{50}(P_{CO_2})$ and $P_{50}([DPG]_{rbc})$ are best-fitted by quadratic polynomials, whereas $P_{50}(T)$ is best-fitted by a cubic polynomial. This is demonstrated through Fig. 1. The combined best-fit polynomial for $P_{50}(pH_{rbc}, P_{CO_2}, [DPG]_{rbc}, T)$ is given by

$$\begin{aligned} P_{50} = {} & 26.8 - 21.279(pH_{rbc} - 7.24) + 8.872(pH_{rbc} - 7.24)^2 \\ & + 0.0482(P_{CO_2} - 40) + 3.64\text{E}-5(P_{CO_2} - 40)^2 \\ & + 795.63([DPG]_{rbc} - 0.00465) \\ & - 19660.89([DPG]_{rbc} - 0.00465)^2 \\ & + 1.4945(T - 37) + 0.04335(T - 37)^2 \\ & + 0.0007(T - 37)^3. \end{aligned} \tag{11}$$

The empirical equation for $P_{50}(pH_{rbc}, P_{CO_2}, T)$ from Kelman's[18] model is given by

$$\begin{aligned} P_{50} = {} & 26.8 \times 10^{\wedge}[0.4(7.24 - pH_{rbc}) \\ & + 0.06 \log(P_{CO_2}/40) + 0.024(T - 37)]. \end{aligned} \tag{12}$$

The $P_{50}(pH_{rbc})$ and $P_{50}(P_{CO_2})$ computed from Eq. (11) are more accurate than those computed from Eq. (12). They agree closely near the standard physiological conditions, but deviate when the conditions are far different from the standard conditions, as seen in Figs. 1a and 1b. The $P_{50}(T)$ formulas agree well over the whole range of T, as seen in Fig. 1d. Kelman did not account for the effect of $[DPG]_{rbc}$.

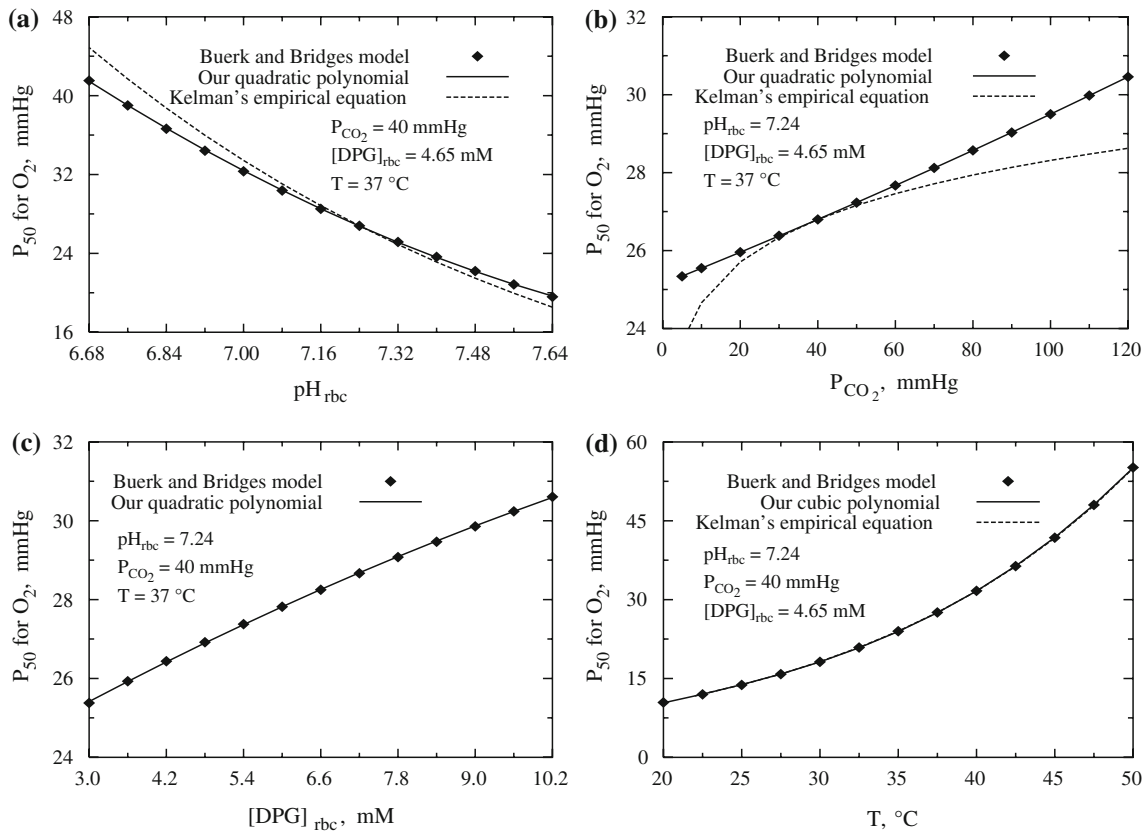

FIGURE 1. The plot of oxygen P_{50} (pH_{rbc}, P_{CO_2}, $[DPG]_{rbc}$, T) with one of the variables varying and the other three fixed at their standard physiological values. The P_{50}'s computed from Buerk and Bridges'[7] model are shown by solid points, from our best-fit polynomial (11) are shown by solid lines, and from Kelman's empirical equation (12) are shown by dashed lines.

Figure 1 shows the variation of P_{50} with pH_{rbc} for $P_{CO_2} = 40$ mmHg, $[DPG]_{rbc} = 4.65$ mM and $T = 37$ °C in panel A; P_{50} with P_{CO_2} for $pH_{rbc} = 7.24$, $[DPG]_{rbc} = 4.65$ mM and $T = 37$ °C in panel B; P_{50} with $[DPG]_{rbc}$ for $pH_{rbc} = 7.24$, $P_{CO_2} = 40$ mmHg and $T = 37$ °C in panel C; and P_{50} with T for $pH_{rbc} = 7.24$, $P_{CO_2} = 40$ mmHg and $[DPG]_{rbc} = 4.65$ mM in panel D. The P_{50} values from the model of Buerk and Bridges[7] are shown by solid points and the corresponding best-fit polynomials are shown by solid lines. The P_{50} values from the model of Kelman[18] are shown by dashed lines. This figure illustrates that the O_2 affinity of Hb decreases (i.e., the P_{50} level increases) as pH decreases (or $[H^+]$ increases) and P_{CO_2}, [DPG] or T increases. Also, the O_2 affinity is significantly affected by the pH and temperature T. The values of P_{50} computed from Eq. (11) are used here to estimate the values of K_4'', n_0, n_1, n_2, n_3 and n_4.

Equations for Parameter Estimation

Now eliminating K_{HbO_2} from Eqs. (7a) and (8a), then substituting the expression for K_4'' from Eq. (9), and finally evaluating the resulting equation at 50% HbO_2 saturation ($S_{HbO_2} = 0.5$), we obtain the following equation relating K_4'', n_0, n_1, n_2, n_3 and n_4 to P_{50}:

$$\frac{K_4'' K_{\text{fact}}}{K_{\text{ratio}}[O_2]_S^{n_0}} = \frac{1}{(\alpha_{O_2} P_{50})^{1+n_0}}, \tag{13}$$

where K_{ratio} and K_{fact} below characterize the nonlinear O_2–CO_2 interactions:

$$K_{\text{ratio}} = \frac{\left(K_2'[CO_2]\left\{1 + \frac{K_2''}{[H^+]}\right\} + \left\{1 + \frac{[H^+]}{K_5''}\right\}\right)}{\left(K_3'[CO_2]\left\{1 + \frac{K_3''}{[H^+]}\right\} + \left\{1 + \frac{[H^+]}{K_6''}\right\}\right)} \tag{14a}$$

$$K_{\text{fact}} = \left\{\frac{[H^+]_S}{[H^+]}\right\}^{n_1} \left\{\frac{[CO_2]_S}{[CO_2]}\right\}^{n_2} \left\{\frac{[DPG]_S}{[DPG]}\right\}^{n_3} \left\{\frac{T_S}{T}\right\}^{n_4}, \tag{14b}$$

$P_{50} = P_{50}$ ($[H^+]$, $[CO_2]$, [DPG], T) on the right hand side of Eq. (13) is based on the model of Buerk and Bridges[7] which is plotted in Fig. 1 and is given by the polynomial (11). We use Eqs. (13), (14a) and (14b) to estimate the values of K_4'', n_0, n_1, n_2, n_3 and n_4.

Estimation of K_4'' and n_0

Now the proportionality equilibrium constant K_4'' and empirical exponent n_0 can be estimated simultaneously by fixing the physiological state variables at their standard values: $[H^+] = [H^+]_S$ (or $pH = pH_S$), $[CO_2] = [CO_2]_S$ (or $P_{CO_2} = P_{O_2}$), $[DPG] = [DPG]_S$, and $T = T_S$. Then Eq. (13) becomes independent of the exponents n_1, n_2, n_3 and n_4 (because all the ratios in K_{fact} are 1) and so depends only on the exponent n_0. On comparing the resulting equation with the relation between the Hill exponent and Hill coefficient (given below Eq. 1), we obtain the following estimations for K_4'' and n_0:

$$K_4'' = \frac{K_{ratio,S}[O_2]_S^{n_0}}{\left(\alpha_{O_2,S}P_{50,S}\right)^{1+n_0}} \quad \text{and} \quad n_0 = 1.7. \tag{15}$$

Under standard physiological conditions in the arterial system, we have $[O_2] = [O_2]_S = 146\ \mu M$ (or $P_{O_2} = P_{O_{2,S}} = 100$ mmHg), $[CO_2] = [CO_2]_S = 1.31$ mM (or $P_{CO_2} = P_{CO_{2,S}} = 40$ mmHg), $[H^+] = [H^+]_S = 57.5$ nM (or $pH = pH_S = 7.24$), $[DPG] = [DPG]_S = 4.65$ mM, and $T = T_S = 37$ °C in RBCs; pH = 7.24 in RBCs corresponds to pH = 7.4 in plasma, because the Gibbs–Donnan ratio R_{rbc} for the electrochemical equilibrium condition across the RBC membrane is about 0.69[14–16,31,38]; the value [DPG] = 4.65 mM corresponds to the ratio [DPG]/[Hb] = 0.9 which is used as the standard ratio by Winslow *et al.*[39] and Buerk and Bridges.[7] Under these conditions, $P_{50} = P_{50,S} = 26.8$ mmHg for human blood,[6,7,39,40] which when substituted into Eq. (15) gives the estimation $K_4'' = 202123\ M^{-1}$ that is independent of the choices of n_1, n_2, n_3 and n_4. It can be noted here that one can use $P_{O_{2,S}} = P_{50,S} = 26.8$ mmHg as the reference P_{O_2} instead of $P_{O_{2,S}} = 100$ mmHg. However, this will give a different estimate of K_4'', while the estimate $n_0 = 1.7$ will remain unchanged.

The current model can be made to fit the Adair model (or Severinghaus's[33] model) by adjusting parameters so that Eqs. (7a), (8a) and (9) fit Adair's equation (or Severinghaus's[33] equation). In this case, the exponent n_0 will be obtained as a function of P_{O_2}. However, we avoid this because the S_{HbO_2} to P_{O_2} relationship will then no longer be analytically invertible. See Appendix A for the calculation of blood O_2 content from saturation, S_{HbO_2}, and P_{O_2}, and see Appendix B for calculating P_{O_2} from S_{HbO_2} and the P_{50}, taking into account P_{CO_2}, pH, [2,3-DPG], *Hct*, and *T*.

Estimation of n_1, n_2, n_3 and n_4

The empirical exponents n_1, n_2, n_3 and n_4 are estimated as independent of each other. These are estimated recursively by varying one of the physiological state variables and fixing the others at their standard values. For example, the exponent n_1 is estimated by varying the level of pH and fixing the levels of P_{CO_2}, [DPG] and T at their standard values $P_{CO_{2,S}}$, $[DPG]_S$ and T_S. In this case, Eq. (13) becomes independent of the exponents n_2, n_3 and n_4 with the pH or $[H^+]$ as the only varying variable. From this resulting equation, the functional expression for n_1 as a function of pH or $[H^+]$ can be obtained. In a similar fashion, the functional expressions for n_2 as a function of P_{CO_2} or $[CO_2]$, n_3 as a function of [DPG], and n_4 as a function of T can also be obtained. These are given by the following exact expressions:

$$n_1(pH_{rbc}) = \frac{\log\left[K_{ratio,1}[O_2]_S^{n_0} \Big/ K_4''\left(\alpha_{O_{2,S}}P_{50,1}\right)^{1+n_0}\right]}{pH_{rbc} - pH_{rbc,S}}, \tag{16a}$$

$$n_2(P_{CO_2}) = \frac{\log\left[K_{ratio,2}[O_2]_S^{n_0} \Big/ K_4''\left(\alpha_{O_{2,S}}P_{50,2}\right)^{1+n_0}\right]}{\log\left(P_{CO_{2,S}}/P_{CO_2}\right)}, \tag{16b}$$

$$n_3([DPG]_{rbc}) = \frac{\log\left[K_{ratio,3}[O_2]_S^{n_0} \Big/ K_4''\left(\alpha_{O_{2,S}}P_{50,3}\right)^{1+n_0}\right]}{\log\left([DPG]_{rbc,S}\big/[DPG]_{rbc}\right)}, \tag{16c}$$

$$n_4(T) = \frac{\log\left[K_{ratio,4}[O_2]_S^{n_0} \Big/ K_4''\left(\alpha_{O_{2,S}}P_{50,4}\right)^{1+n_0}\right]}{\log(T_S/T)}, \tag{16d}$$

where the P_{50}'s are given by the polynomial expression (11) and the second subscript "1", "2", "3" or "4" indicates that a particular one of the variables pH_{rbc}, P_{CO_2}, $[DPG]_{rbc}$ or T is varying.

Figure 2 shows the variation of n_1 with pH_{rbc} for $P_{CO_2} = 40$ mmHg, $[DPG]_{rbc} = 4.65$ mM and $T = 37$ °C in panel A; n_2 with P_{CO_2} for $pH_{rbc} = 7.24$, $[DPG]_{rbc} = 4.65$ mM and $T = 37$ °C in panel B; n_3 with $[DPG]_{rbc}$ for $pH_{rbc} = 7.24$, $P_{CO_2} = 40$ mmHg and $T = 37$ °C in panel C; and n_4 with T for $pH_{rbc} = 7.24$, $P_{CO_2} = 40$ mmHg and $[DPG]_{rbc} = 4.65$ mM in panel D. It is depicted that the exponent n_4 is considerably larger compared to the other exponents n_1, n_2 and n_3, whereas the exponent n_2 is very small. This is because the effect of temperature T on the O_2 affinity is very significant and that of P_{CO_2} is relatively small. These calculated functional forms of the exponents n_1, n_2, n_3 and n_4 are used here to compute S_{HbO_2}, S_{HbCO_2}, $[O_2]_{bl}$ and $[CO_2]_{bl}$. However, for simplicity, the standard values $n_{1,S} = 1.06$, $n_{2,S} = 0.12$, $n_{3,S} = 0.37$, and

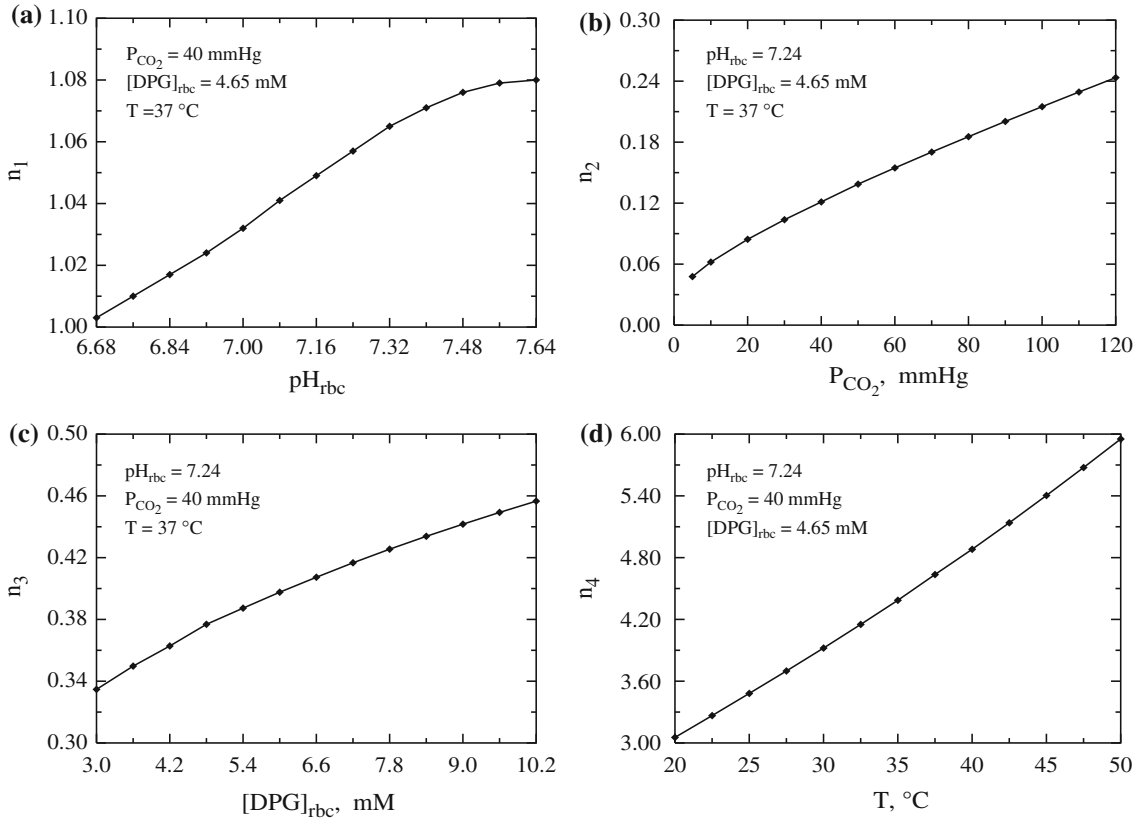

FIGURE 2. The exponents for Eq. (9); the plots of $n_1(pH_{rb\ c})$, $n_2(P_{CO_2})$, $n_3([DPG]_{rbc})$ and $n_4(T)$ with the other three variables fixed at their standard physiological values. These are computed from Eqs. (16a)–(16d) using the estimated value of K_4'' and n_0 and the best-fit polynomial (11) for oxygen P_{50}.

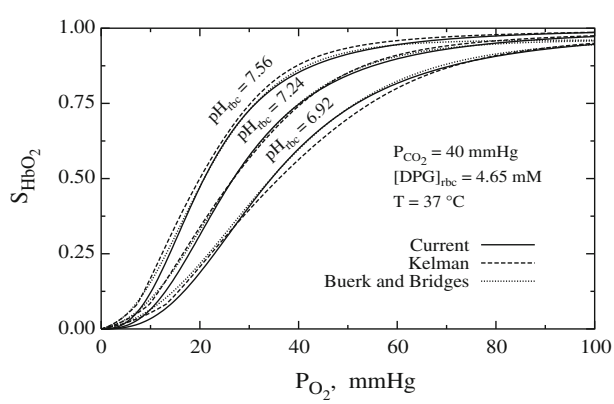

FIGURE 3. The comparison of the HbO_2 dissociation curves computed from our model, Kelman[18] model, and Buerk and Bridges[7] model for different values of pH_{rbc} with P_{CO_2}, $[DPG]_{rbc}$ and T fixed at their standard physiological values.

$n_{4,S} = 4.65$ (see Table 1; calculated using the standard physiological conditions) can also be used. In this case, the shifts in the HbO_2 saturation curves will not be very accurate. The results are summarized through Figs. 3–6, presented below.

DISSOCIATION CURVES AND BLOOD GAS CONTENTS

Oxyhemoglobin (HbO_2) Dissociation Curves

Figure 3 shows the comparison of the HbO_2 dissociation curves computed from current model, Kelman[18] model and Buerk and Bridges[7] model for $pH_{rbc} = 6.92$, 7.24 and 7.56 with $P_{CO_2} = 40$ mmHg, $[DPG]_{rbc} = 4.65$ mM and $T = 37$ °C. It is seen that these curves are in fairly good agreement with each other over the entire saturation range, although our curves are consistently slightly below the curves of Kelman and Buerk and Bridges when $S_{HbO_2} < 30\%$. In this range, our curves are not very accurate, since our model is based on the Hill's equation, which is considered to be accurate only in the saturation range of 20 to 98%,[29] and one might therefore prefer their models at very low P_{O_2} even though inversion is more difficult. However, for $S_{HbO_2} > 30\%$, our curves agree closely with the curves of Buerk and Bridges which were fit to actual human and dog blood HbO_2 saturation data of Roughton *et al.*,[28] Roughton and Severinghaus,[30] Winslow *et al.*,[40] and Sveringhaus.[33]

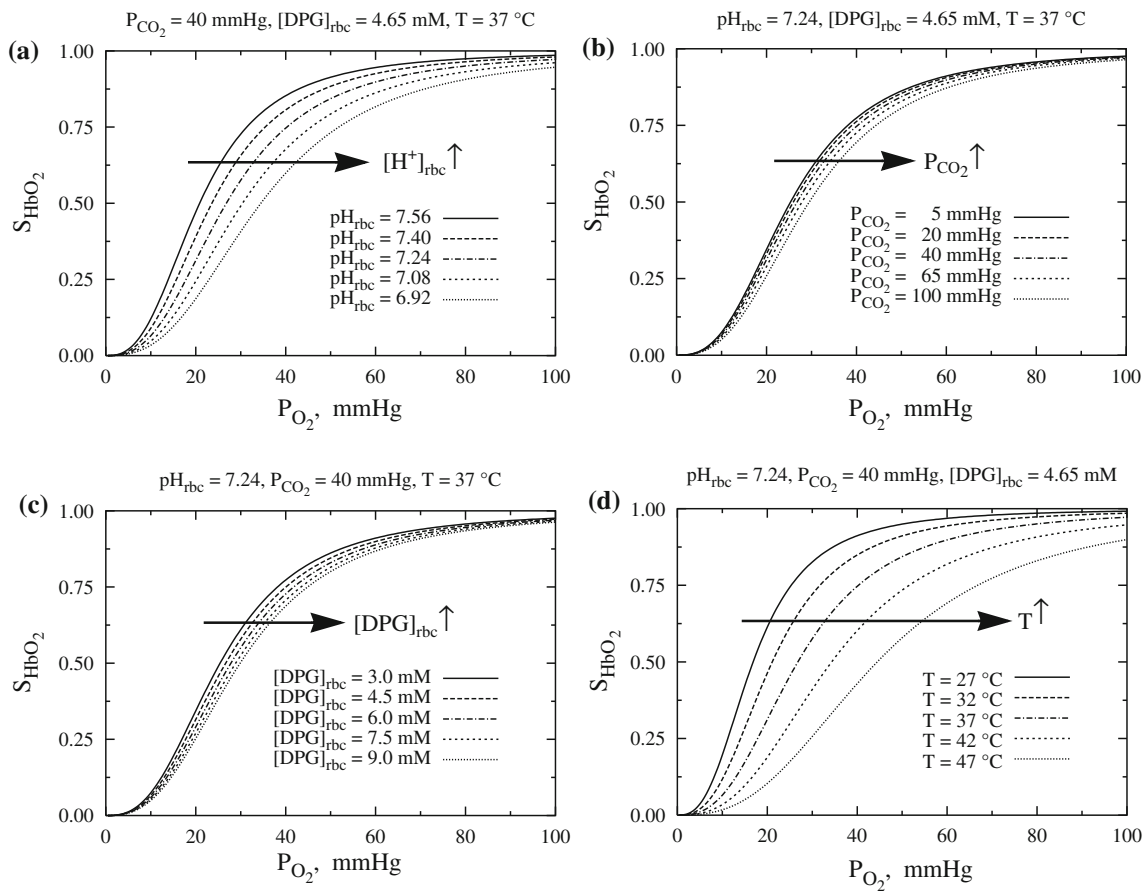

FIGURE 4. The quantitative behavior of the HbO_2 dissociation curves at various physiological conditions (i.e., with varying levels of pH_{rbc}, P_{CO_2}, $[DPG]_{rbc}$ and T) as computed from Eqs. (7a), (8a), (9), (15), and (16a)–(16d).

Also Kelman's model does not give accurate shifts in HbO_2 dissociation curves when physiological variables deviate far from their standard values.

Figure 4 shows the variation of S_{HbO_2} with P_{O_2} for different values of pH_{rbc} with $P_{CO_2} = 40$ mmHg, $[DPG]_{rbc} = 4.65$ mM and $T = 37$ °C in panel A; different values of P_{CO_2} with $pH_{rbc} = 7.24$, $[DPG]_{rbc} = 4.65$ mM and $T = 37$ °C in panel B; different values of $[DPG]_{rbc}$ with $pH_{rbc} = 7.24$, $P_{CO_2} = 40$ mmHg and $T = 37$ °C in panel C; and different values of T with $pH_{rbc} = 7.24$, $P_{CO_2} = 40$ mmHg and $[DPG]_{rbc} = 4.65$ mM in panel D. The HbO_2 dissociation curve shifts to the right (i.e., the P_{50} for O_2 increases, or O_2 affinity of Hb decreases) as pH decreases (or $[H^+]$ increases) and P_{CO_2}, [DPG] or T increases. This diminution of Hb affinity for O_2 as pH decreases or P_{CO_2} increases is known as the Bohr effect, so our model provides a quantitative description of the Bohr effect. The shifts in the HbO_2 dissociation curve with changes in P_{CO_2} or [DPG] are small as compared to those occurring with changes in pH and T; the O_2 affinity of Hb is most sensitive to temperature T. Undoubtedly the fit of these models to complete data sets (such as the unfortunately unavailable set of Winslow *et al.*[40] would result in improved parameter estimates, but these curves should be accurate roughly to 2 or 3% for P_{CO_2}'s above 20 mmHg.

Carbamino-Hemoglobin ($HbCO_2$) Dissociation Curves

Figure 5 shows the variation of S_{HbCO_2} with P_{CO_2} for different values of pH_{rbc} with $P_{O_2} = 100$ mmHg, $[DPG]_{rbc} = 4.65$ mM and $T = 37$ °C in panel A; different values of P_{O_2} with $pH_{rbc} = 7.24$, $[DPG]_{rbc} = 4.65$ mM and $T = 37$ °C in panel B; different values of $[DPG]_{rbc}$ with $pH_{rbc} = 7.24$, $P_{O_2} = 100$ mmHg and $T = 37$ °C in panel C; and different values of T with $pH_{rbc} = 7.24$, $P_{O_2} = 100$ mmHg and $[DPG]_{rbc} = 4.65$ mM in panel D. It is seen that the behavior of the $HbCO_2$ dissociations curves (hyperbolic) is quite different than the HbO_2 dissociation curves (sigmoid). Also, at fixed values of P_{O_2}, P_{CO_2}, pH, [DPG] and T, the Hb saturation of CO_2 (S_{HbCO_2}) is considerably lower than the Hb saturation of O_2 (S_{HbO_2}). This is because the CO_2 binding to Hb is noncooperative in nature,[2] whereas the O_2 binding to Hb is cooperative.

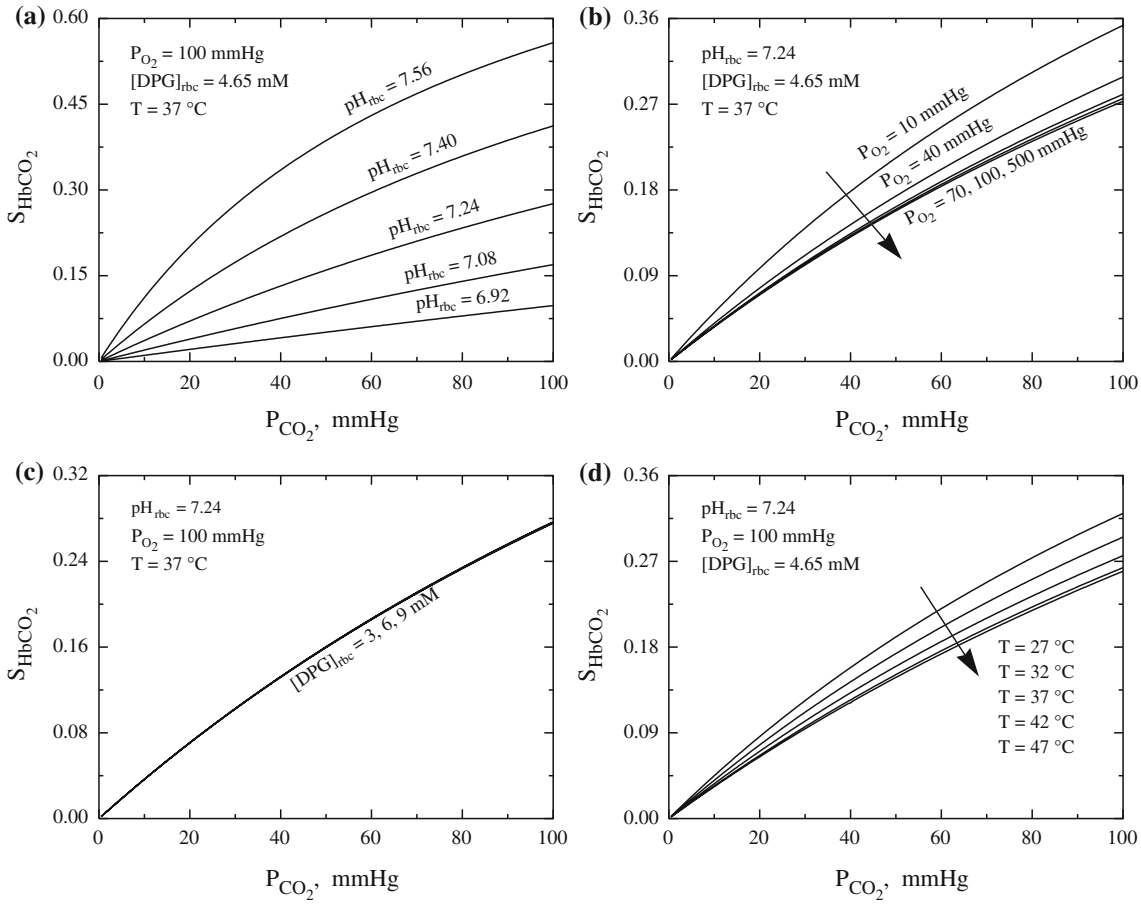

FIGURE 5. The quantitative behavior of the $HbCO_2$ dissociation curves at various physiological conditions (i.e., with varying levels of pH_{rbc}, P_{O_2} $[DPG]_{rbc}$ and T) as computed from Eqs. (7b), (8b), (9), (15), and (16a)–(16d).

Figure 5a depicts that the CO_2 saturation of Hb (S_{HbCO_2}) is greatly affected by pH, and is dependent only on the shift in affinity for single site binding. But raising $[H^+]$, reducing pH, greatly reduces the CO_2 affinity for Hb, reducing the carbamino formation: so the P_{50} for CO_2 shifts rightward. Likewise, Figs. 5b and 5d show that raising P_{O_2} and T shift the P_{50} for CO_2 rightward, indicating a reduction in carbamino formation and CO_2 affinity for Hb. This shift in P_{50} for CO_2 is higher at lower values of P_{O_2} and T and negligible at higher values of P_{O_2} and T. The alteration of the CO_2 affinity of Hb with respect to P_{O_2} is known as the Haldane effect, so our model provides a quantitative description of the Haldane effect.

The curve of S_{HbCO_2} asymptotes at high P_{O_2} to a limiting curve (Fig. 5b) because HbO_2 saturation is almost complete by P_{O_2} = 100 mmHg beyond which O_2 has no direct effect on CO_2 binding. For temperature (Fig. 5d), the apparent asymptotic behavior is due to a combination of factors: a reduction in the concentration of dissolved CO_2 due a decrease in solubility of CO_2 and an increase in the apparent Hill coefficient K_{HbCO_2} due to a decrease in HbO_2 saturation. These opposing trends in $[CO_2]$ and K_{HbCO_2} with raising T diminish the shift in the $HbCO_2$ dissociation curves. Figure 5c depicts that the effect of $[DPG]_{rbc}$ on the CO_2 affinity of Hb can be neglected, as K_{HbCO_2} and K_{HbCO_2} are almost independent of $[DPG]_{rbc}$.

CO_2 Content in Whole Blood, $[CO_2]_{bl}$

Figure 6 shows the variation of $[CO_2]_{bl}$ (ml of CO_2 per 100 mL of blood) with P_{CO_2}, for different values of P_{O_2} and $[DPG]_{rbc}$ with pH_{rbc} = 7.24, T = 37 °C, and Hct = 0.45 in panel A; for different values of pH_{rbc} with T = 37 °C, Hct = 0.45, and all P_{O_2} and $[DPG]_{rbc}$ in panel B; for different values of T with pH_{rbc} = 7.24, Hct = 0.45, and all P_{O_2} and $[DPG]_{rbc}$ in panel C; and for different values of *Hct* with pH_{rbc} = 7.24, T = 37 °C, and all P_{O_2} and $[DPG]_{rbc}$ in panel D. Generally $[CO_2]_{bl}$ varies linearly with P_{CO_2}, and varies negligibly with P_{O_2} and $[DPG]_{rbc}$. This is because most

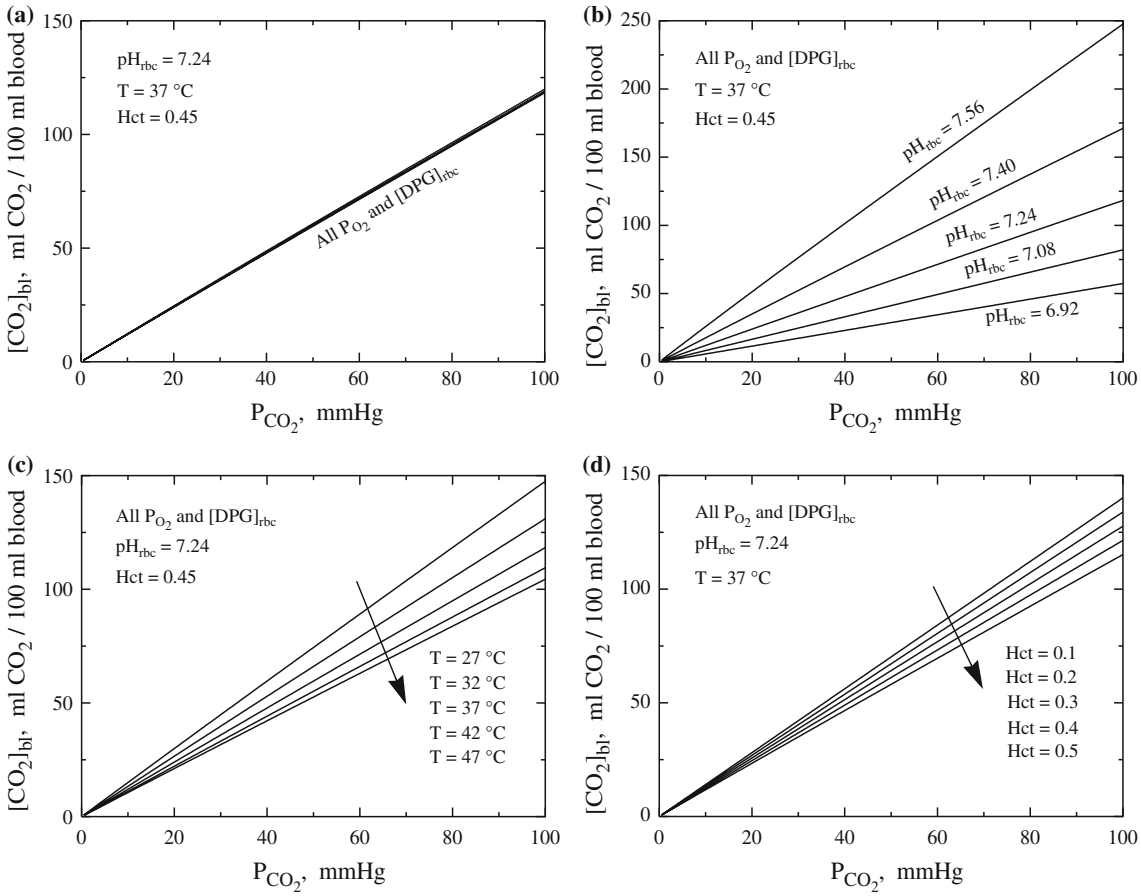

FIGURE 6. Total CO_2 content of whole blood ($[CO_2]_{bl}$, mL CO_2 per 100 mL blood) as a function of P_{CO_2} at various physiological conditions (i.e., with varying levels of pH_{rbc}, P_{O_2}, $[DPG]_{rbc}$, *T* and *Hct*) as computed through Eqs. (A.2) and (A.3).

of the CO_2 is carried as bicarbonate, and very little in the form of carbamino. Figure 6b shows that the $[CO_2]_{bl}$ decreases as pH decreases and $[HCO_3^-]$ decreases, by Eq. (A.3). An increase in the temperature T (Fig. 6c) reduces the CO_2 solubility and leads to a decrease in $[CO_2]$ and then $[HCO_3^-]$. Figure 6d shows that an increase in *Hct* leads to a decrease of plasma space, an increase in average pH in blood (since $pH_{rbc} = 7.24$ and $pH_{pl} = 7.4$), and hence a decrease in $[HCO_3^-]$. These lead to a decrease in total CO_2 content in whole blood.

DISCUSSION AND CONCLUSIONS

The transport and exchange of O_2 and CO_2 in the circulatory system is highly influenced by the competitive binding of O_2 and CO_2 with hemoglobin (i.e., the Hb-mediated nonlinear O_2–CO_2 interactions) and by the levels of pH (acidity), 2,3-DPG concentration, and temperature in RBCs. Thus, in the modeling of simultaneous transport and exchange of O_2 and CO_2, one must consider suitable model equations for O_2 and CO_2 saturations of Hb (S_{HbO_2} and S_{HbCO_2}) which are coupled or linked to each other through the kinetics of O_2 and CO_2 binding to Hb. Also, for computational efficiency, in simulating the blood-tissue gas exchange processes in changing physiological states, the S_{HbO_2} to P_{O_2} and S_{HbCO_2} to P_{CO_2} relationships should be analytically invertible. Again, since the S_{HbO_2} is measurable spectrophotometrically, estimating P_{O_2} from S_{HbO_2} is of practical, even clinical, consequence. However, as S_{HbCO_2} can not currently be estimated spectrophotometrically, there is no practical utility in calculating P_{CO_2} from S_{HbCO_2}.

The models for standard HbO_2 dissociation curve, valid for only fixed/standard values of pH, P_{CO_2}, [DPG]/[Hb] and T,[1,6,8,13] are not very efficient to use in the simulation of dynamic blood–tissue gas exchange processes. To make them applicable, one must multiply all P_{O_2} values of the standard curve by a factor which is composite for the variations in pH, P_{CO_2}, [DPG] and T (e.g., as in Kelman[18] and Severinghaus[33]). The numerical algorithm of Winslow *et al.*[39] for computing the nonstandard HbO_2 dissociation curves is very complicated, because it needs numerical evaluation of

all the four Adair constants as functions of pH, P_{CO_2} and [DPG]/[Hb] by fitting the Adair's equation with the experimental data on HbO_2 saturation in human whole blood. Their quadratic fit regression analysis for the four Adair constants needs numerical evaluation of a total of 72 coefficients. The effect of temperature (T) were not established, but would need an estimation of 24 additional coefficients to extend their algorithm. Like Adair's equation, the empirical equations of Kelman[18] and Siggaard-Andersen *et al.*[37] for nonstandard HbO_2 dissociation curves require numerical inversion for computing P_{O_2} from S_{HbO_2}, which is computationally expensive. The model of Buerk and Bridges,[7] being analytically invertible, is more efficient. However, it does not describe the upper 5% of the dissociation curve accurately. Besides, all these models of HbO_2 dissociation curves need a suitable coupled model of $HbCO_2$ dissociation curves for integrating into a computational model of simultaneous or dynamic O_2 and CO_2 transport and exchange in the microcirculation.

The model of Singh *et al.*[38] for nonstandard HbO_2 and $HbCO_2$ dissociation curves is based on the equilibrium binding of O_2 and CO_2 with Hb, but it does not account for the effects of 2,3-DPG concentration and temperature in blood. Also Singh *et al.*'s estimates of the equilibrium constants for the kinetic reactions do not agree well with the experimental values reported earlier.[2,10,11,14–16,29,31] Their formulation for kinetic reactions of O_2 and CO_2 with Hb was based on the assumption that the Hb molecule has only one heme-amino chain, Hm-NH_2, and is capable of binding to only one CO_2 molecule, and therefore requires correction, since Hb actually has four Hm-NH_2 chains and can bind to four CO_2 molecules.

In an attempt to address these issues, a more appropriate and relatively simple mathematical model equations (Eqs. 7a and 7b) for O_2 and CO_2 saturations of Hb (S_{HbO_2} and S_{HbCO_2}) are developed in this paper. These are derived by considering the equilibrium binding of O_2 and CO_2 with Hb inside RBCs,[2,14,29,31,38] including the Hb-mediated nonlinear O_2–CO_2 interactions and the effects of pH, 2,3-DPG, and temperature. Unlike in the previous models mentioned above, Hb molecule is considered to have four heme-amino chains, Hm-NH_2, each capable of binding to one O_2 molecule and one CO_2 molecule. The binding of O_2 is considered to be cooperative and that of CO_2 as non-cooperative. The new model equations for S_{HbO_2} and S_{HbCO_2} are of the form of Hill's equation, which has the extra advantage of being analytically invertible, allows the O_2 and CO_2 partial pressures (P_{O_2} and P_{CO_2}) to be computed directly from their saturations (S_{HbO_2} and S_{HbCO_2}) and vice versa (see Appendix B). However, this new model is highly accurate only above 30% (S_{HbO_2} or a P_{O_2} of 20 mmHg, and leads to 1 to 2% underestimation of the saturation from the P_{O_2} in computing intracapillary profiles of O_2 and CO_2 from models of simultaneous transport and exchange of O_2 and CO_2. Improvement is needed here, though the low range is not very commonly encountered in normal circumstances; the Severinghaus[33] model would be an improvement within the range of conditions covered by that model.

The apparent Hill coefficients K_{HbO_2} and K_{HbCO_2} in the expressions for S_{HbO_2} and S_{HbCO_2} (Eqs. 8a and 8b) are explicitly dependent on the levels of P_{O_2}, P_{CO_2}, pH, [2,3-DPG] and T in RBCs and are dependent on the equilibrium constants of the chemical reactions involved in the binding O_2 and CO_2 with Hb. So these establish the linkage between S_{HbO_2} and S_{HbCO_2} and the nonlinear O_2–CO_2 interactions. The cooperativity of O_2 binding and the effects of nonstandard physiological conditions are established in this model by considering the equilibrium constant for the reaction of O_2 with an Hm-NH_2 chain as a suitable function of P_{O_2}, P_{CO_2}, pH, [2,3-DPG] and T involving six adjustable parameters (see Eq. 9), including one proportionality equilibrium constant K_4'' and five empirical exponents n_0, n_1, n_2, n_3 and n_4. These were estimated using the P_{50} (pH_{rbc} P_{CO_2} $[DPG]_{rbc}$ T) values from the model of Buerk and Bridges[7] for nonstandard HbO_2 dissociation curves which agree closely with those obtained theoretically by Kelman[18] and experimentally by Winslow *et al.*[39] for normal human whole blood. These estimates are also influenced by the equilibrium constants for the other kinetic reactions in the uptake of CO_2 and ionization of Hm-NH_2 chains. These equilibrium constants are chosen or calculated appropriately to be consistent with those referred to largely in the literature.[2,14–16,31]

Our new model could be fitted to other sets of experimental data for characterizing the O_2 and CO_2 saturation of Hb. The report of Winslow *et al.*[39] was based on a large dataset, and in their report, the data were summarized by the P_{50} values; the original data are no longer available, unfortunately, else they would have served as an excellent test of our descriptive equations. From an optimization using such large datasets, we would obtain more precise estimates of equilibrium constants and P_{50} (pH_{rbc}, P_{CO_2}, $[DPG]_{rbc}$, T) values, and presumably improved estimates of our model parameters, particularly the exponents n_1, n_2, n_3 and n_4.

The new model equations for S_{HbO_2} and S_{HbCO_2} are used here to calculate the O_2 and CO_2 contents in whole blood (see Appendix A). The HbO_2 and $HbCO_2$ dissociation curves and the O_2 and CO_2 contents in whole blood computed through these new equations are in good agreement with the published experimental and theoretical results in the literature. The result

shows that at normal physiological conditions in arterial blood, the P_{O_2} is about 100 mmHg and so Hb is about 97.2% saturated by O_2 while the amino group of Hb is about 13.1% saturated by CO_2. The invertibility (see Appendix B) of our new equations for S_{HbO_2} and S_{HbCO_2} allows their convenient use in computationally complex models of simultaneous or dynamic transport and exchange of O_2 and CO_2 in the alveoli–blood and blood–tissue exchange systems. This model has been implemented in our Java Simulation (JSim) interface, the mathematical modeling language (MML) code of which is available for download and public use at our physiome website, http://physiome.org/Models/GasTransport.

Our new model is unique in the sense that it is derived from the equilibrium binding of O_2 and CO_2 with Hb and it accounts for all the factors (e.g., P_{O_2}, P_{CO_2}, pH, [DPG] and T) that affect the O_2 and CO_2 binding to Hb. It also establishes the linkage between S_{HbO_2} and S_{HbCO_2} as well as the Hb-mediated nonlinear O_2–CO_2 interactions (or Bohr and Haldane effects), the effects of which are important in simulating the complex simultaneous or dynamic transport and exchange of O_2 and CO_2 in the microcirculation. The kinetic and equilibrium constants, compiled from the literature or estimated in this paper, can be used in the dynamically modeling of the complex gas exchange process in vivo. These can also used to compute the concentrations of all the reaction products at equilibrium from Eqs. (3a) to (3i).

In summary, our new multidimensional model equations for S_{HbO_2} and S_{HbCO_2} are relatively simple, lending themselves to simple equation-solving by spreadsheet or by a simple program in a handheld computer. Severinghaus[32] provided a slide rule for this purpose, and later in his 1979 paper,[33] he summarized all the earlier calculations through appropriate model equations, which gives the earlier references, and which stimulated Ellis[9] to provide the inverted calculation (P_{O_2} from S_{O_2}). The Appendix B provides a recipe for the inversion of our new S_{HbO_2} to P_{O_2} relationship that allows calculation of whole blood O_2 content from the HbO_2 saturation (e.g., provided spectrophotometrically) and other chemically or physically determined measures of pH, P_{O_2} P_{CO_2} or bicarbonate, [2,3-DPG], and temperature (T) in blood. Of particular value in analyzing the ^{15}O-oxygen time course data from PET (positron emission tomography) using convection–diffusion distributed models (e.g., Li *et al.*[23] is the analytical invertibility of the Hill-type expression for S_{HbO_2}, as given by Eqs. (B.1) to (B.3) in the Appendix B.

We measured the computation times for numerical inversion of Kelman's[18] equation. It took 20–25 times more computer time (because of the numbers of iterations required) than the analytical inversion of Hill's equation for computing P_{O_2} from S_{HbO_2}. This is more significant in the convection–diffusion distributed modeling of O_2 and CO_2 transport in blood–tissue exchange systems which involves large number of spatial and temporal grid points. Again, in the estimation of parameters, using such axially distributed models, accounting for the gradients in [O_2], [CO_2], pH and T along the capillary length, will require another level of iteration during the optimization process: this means that computational efficiency is doubly important.

APPENDIX A

Calculation of O_2 Content in Whole Blood

To calculate the O_2 content of whole blood, we need to sum the two forms of O_2 in blood: O_2 dissolved in plasma water and RBC water and O_2 as oxyhemoglobin in RBCs. Thus, the molar O_2 concentration of whole blood, $[O_2]_{bl}$, can be calculated as

$$[O_2]_{bl} = W_{bl}\alpha_{O_2}P_{O_2} + 4[Hb]_{bl}S_{HbO_2}, \qquad (A.1)$$

where W_{bl} is the fractional water space of blood and is related to that of plasma and RBCs (W_{pl} and W_{rbc}) by $W_{bl} = (1 - Hct)\ W_{pl} + Hct\ W_{rbc}$; $[Hb]_{bl}$ is the molar concentration of hemoglobin in whole blood and is related to that in RBCs, $[Hb]_{rbc}$, by $[Hb]_{bl} = Hct\ [Hb]_{rbc}$; Hct is the blood hematocrit. It is assumed that the O_2 partial pressures in plasma and RBCs are equal. The factor 4 in Eq. (A.1) indicates that four molecules of O_2 bind to one molecule of Hb. The whole blood O_2 content in mL of O_2 per mL of blood is 22.256 times $[O_2]_{bl}$.

At standard physiological conditions, Hct is about 0.45 and $[Hb]_{bl}$ is about 0.15 g/mL or 2.33 mM taking the molecular weight of Hb to be 64,458.[19] Correspondingly, $[Hb]_{rbc}$ is about 5.18 mM that is assumed to be fixed and independent of Hct. With $W_{pl} = 0.94$, $W_{rbc} = 0.65$ and $Hct = 0.45$, we have $W_{bl} = 0.81$ mL water per mL blood. With these data and at a P_{O_2} of 100 mmHg, the O_2 saturation of Hb, S_{HbO_2}, is about 97.2%, the O_2 content of whole blood is about 0.26 mL O_2 per 100 mL blood in free form plus about 20.18 mL O_2 per 100 mL blood bound to Hb, making a total O_2 content in whole blood of 20.44 mL O_2 per 100 mL blood.

Calculation of CO_2 Content in Whole Blood

To calculate the CO_2 content of whole blood, we need to sum the four forms of CO_2 in blood: CO_2 in dissolved form, as carbonic acid (H_2CO_3), as

bicarbonate ions (HCO_3^-), and as carbamino-hemoglobin ($HbCO_2$). The dissociation constant K_1'' for H_2CO_3 is about 5.5×10^{-4} M[14–16] while the concentration of H^+ in plasma is about 3.98×10^{-8} M and in RBCs is about 5.75×10^{-8} M. So the concentration of H_2CO_3 is usually four orders of magnitude smaller than that of (HCO_3^-). Therefore, its contribution to the CO_2 content can be neglected.

Again four moles of CO_2 bind with one mole of Hb in RBCs. So with the assumption that the CO_2 partial pressures in plasma and RBCs are equal, the molar CO_2 concentration of whole blood, $[CO_2]_{bl}$, can be calculated as

$$[CO_2]_{bl} = W_{bl}\alpha_{CO_2}P_{CO_2} + \left[HCO_3^-\right]_{bl} + 4[Hb]_{bl}S_{HbCO_2}, \tag{A.2}$$

where the total bicarbonate in blood, $[HCO_3^-]_{bl}$, is obtained by using the Henderson-Hasselbalch equation and Gibbs–Donnan electrochemical equilibrium condition as:

$$\begin{aligned}\left[HCO_3^-\right]_{bl} &= (1 - Hct)W_{pl}\left[HCO_3^-\right]_{pl} + Hct\,W_{rbc}\left[HCO_3^-\right]_{rbc} \\ &= \left\{(1 - Hct)W_{pl} + Hct\ W_{rbc}R_{rbc}\right\}\left\{\frac{K_1\alpha_{CO_2}P_{CO_2}}{[H^+]_{pl}}\right\}.\end{aligned} \tag{A.3}$$

Here $K_1 = K_1'K_1''$ is the equilibrium constant for overall CO_2 hydration reaction (2a) and $R_{rbc} = [H^+]_{pl}/H^+]_{rbc} = [HCO_3^-]_{rbc}/[HCO_3^-]_{pl}$ is the Gibbs–Donnan ratio for electrochemical equilibrium condition across the RBC membrane. The value of R_{rbc} is about 0.69.[14–16,31,38] Multiplying $[CO_2]_{bl}$ by 22.256 converts the units of molar to mL of CO_2 per mL of blood.

From the data used in Hill *et al.*,[14–16] $[H_2O]\,kf_1' \approx 0.12\ s^{-1}$ and $kb_1' \approx 89\ s^{-1}$, so $K_1' = [H_2O]kf_1'/kb_1' \approx 1.35 \times 10^{-3}$. Again, $K_1'' \approx 5.5 \times 10^{-4}$ M, so $K_1 = K_1'K_1'' \approx 7.43 \times 10^{-7}$ M, as shown in Table 1. Thus, $pK_1 = -\log(K_1) \approx 6.13$, which is close to the standard value $pK_1 = 6.1$ reported in text books and literature. However, pK_1 depends on the levels of pH and temperature T in plasma. This dependency was expressed by the following curve-fit equation by Kelman[21] based on the experimental data of Austin *et al.*[3]:

$$\begin{aligned}pK_1 = 6.09 &- 0.0434(pH_{pl} - 7.4) \\ &+ 0.0014(T - 37)(pH_{pl} - 7.4).\end{aligned} \tag{A.4}$$

At $pH_{pl} = 7.4$ and $T = 37$, Eq. (A.4) gives $pK_1 = 6.09$ which is close to the value $pK_1 = 6.13$ calculated above and agrees well with the data of Severinghaus *et al.*[35]

At standard physiological conditions, the CO_2 content of whole blood in free form is about 2.35 mL CO_2 per 100 mL blood (i.e., 1.06 mM), in bicarbonate form is about 42.69 mL CO_2 per 100 mL blood (i.e., 19.18 mM), and in carbamino form is about 2.72 mL CO_2 per 100 mL blood (i.e., 1.22 mM), making a total CO_2 content in whole blood of 47.76 mL CO_2 per 100 mL blood (i.e., 21.45 mM). These estimates agree with the data reported in the literature.[21,22,29] The CO_2 saturation of Hb, S_{HbCO_2}, is computed to be about 13.1% at a P_{CO_2} of 40 mmHg.

APPENDIX B

Algorithm for Inverting the Relationships Between S_{HbO_2} and P_{O_2}

Equation (7a) for the fractional saturation S_{HbO_2} is not convenient for analytical inversion because the apparent Hill coefficient K_{HbO_2} depends on $[O_2]$ (see Eq. 8a). However, with the help of Eq. (9), the expression for S_{HbO_2} can be rewritten in the following form, which is amenable for analytical inversion:

$$S_{HbO_2} = \frac{K'_{HbO_2}[O_2]^{1+n_0}}{1 + K'_{HbO_2}[O_2]^{1+n_0}}, \tag{B.1}$$

where K'_{HbO_2} (with units $M^{-(1+n_0)}$) is given by Eqs. (13) and (14):

$$K'_{HbO_2} = \frac{K_4''K_{fact}}{K_{ratio}[O_2]_S^{n_0}} = \frac{1}{(\alpha_{O_2}P_{50})^{1+n_0}}. \tag{B.2}$$

The P_{50} is defined as before by Eq. (11) and the kinetic terms K_{ratio} and K_{fact} are defined by Eqs. (14a) and (14b). The Hill exponent in the expression for S_{HbO_2} is now $1 + n_0$ and apparent Hill coefficient K'_{HbO_2} is now independent of $[O_2]$. This makes S_{HbO_2} analytically invertible, when P_{CO_2}, pH, [DPG] and T are known. The inverted equation for $[O_2]$ is given by

$$[O_2] = \left[\frac{S_{HbO_2}}{K'_{HbO_2}(1 - S_{HbO_2})}\right]^{\frac{1}{1+n_0}} = \alpha_{O_2}P_{50}\left[\frac{S_{HbO_2}}{1 - S_{HbO_2}}\right]^{\frac{1}{1+n_0}}. \tag{B.3}$$

It is clear from Eq. (B.2) that K'_{HbO_2} can be determined completely using only the $P_{50} = P_{50}$ ($[H^+]$, $[CO_2]$, [DPG], T) data which is given by Eq. (11). This avoids the calculations of K_{ratio} and K_{fact} which involves the complex computations of the empirical indices n_1, n_2, n_3, and n_4 using Eqs. (16a) to (16d). This also simplifies the computation of S_{HbO_2} from $[O_2]$ and vice versa significantly. However, in the computation of S_{HbCO_2} from $[CO_2]$ and vice versa (not shown in this

appendix), the calculations of K_{fact} and K_{ratio} are essential as the P_{50} data for 50% $HbCO_2$ saturation is not available in the literature.

Here Eq. (B.1) further suggests that, in nonstandard physiological conditions, S_{HbO_2} can be computed from the original Hill's equation (Eq. 1) by scaling the $[O_2]$ axis by a factor $1/K'_{HbO_2}$ (see Eq. B.2) which is composite for the variations in pH, P_{CO_2}, [2,3-DPG], and temperature (T), as in Kelman[18] and Severinghaus.[33] The same conclusion is valid for the computation of S_{HbCO_2} from $[CO_2]$.

The inversion procedure for determining P_{O_2} and then total O_2 content in whole blood from the observations on S_{HbO_2}, P_{CO_2}, pH_{pl}, $[DPG]_{bl}$, Hct, and T in blood is as follows:

A. Calculate $[H^+]_{pl} = 10^{-pH_{pl}}$, $[H^+]_{rbc} = [H^+]_{pl}/R_{rbc}$, $pH_{rbc} = -\log[H^+]_{rbc}$, and $[DPG]_{rbc} = [DPG]_{bl}/Hct$, where $R_{rbc} = 0.69$.
B. Calculate $P_{50} = P_{50}\,(P_{CO_2}, pH_{rbc}, [DPG]_{rbc}, T)$ from Eq. (11).
C. Calculate $[O_2]$ from Eq. (B.3), and then $P_{O_2} = [O_2]/\alpha_{O_2}$, where α_{O_2} is given by Eq. (10a), and n_0 is 1.7. This is the inversion step.
D. Calculate $[Hb]_{bl} = Hct \times [Hb]_{rbc} = Hct \times 5.18$ mM, assuming that the RBC has standard hemoglobin concentration of 5.18 mM and that there is no methemoglobin or other abnormal type of hemoglobin.
E. Calculate $W_{bl} = W_{pl}\,(1 - Hcts) + W_{rbc}\,Hct = 0.94\,(1 - Hct) + 0.65\,Hct$, as the fractional water content of blood.
F. Calculate $[O_2]_{bl} = W_{bl}\,[O_2]_{bl} + 4\,[Hb]_{bl}\,S_{HbO_2}$, as the total O_2 content in whole blood in M. To convert from $[O_2]_{bl}$ M to mL gaseous O_2 per mL blood, use mL O_2 gas/100 mL blood $= 22{,}256 \times 100/1000 \times [O_2]_{bl} = 2225 \times [O_2]_{bl}$.

This procedure can be set up in a spreadsheet, programmable hand calculator, or in any computer program such as the JSim MML code (available from the website http://www.physiome.org/Models/GasTransport/ for Linux, Unix, Macintosh and Windows). JSim, the general modeling system, and extensive manuals for it, can be downloaded from http://www.physiome.org/jsim/ for free.

ACKNOWLEDGMENTS

This research was supported by the National Simulation Resource for Circulatory Mass Transport and Exchange via grants NCRR/NIH P41-RR1243 and NIBIB/NIH R01-EB001973. The authors are grateful to the referees for their comments and suggestions, and to John Kenneth Baillie, University of Edinburgh for corrections to Eq. (11) of the 2004 publication.

REFERENCES

[1]Adair, G. S. The hemoglobin system. VI. The oxygen dissociation curve of hemoglobin. *J. Biol. Chem.* 63:529–545, 1925.
[2]Antonini, E., and M. Brunori, *Hemoglobin and Myoglobin in Their Reactions with Ligands*, Amsterdam: North Holland, 436 pp, 1971.
[3]Austin, W. H., E. Lacombe, P. W. Rand, and M. Chatterjee. Solubility of carbon dioxide in serum from 15 to 38°C. *J. Appl. Physiol.* 18:301–304, 1963.
[4]Bauer, C., R. A. Klocke, D. Kamp, and R. E. Forster. Effect of 2,3-diphosphoglycerate and H+ on the reaction of O_2 and hemoglobin. *Am. J. Physiol.* 224:838–847, 1973.
[5]Baumann, R., H. Bartels, and C. Bauer. Blood oxygen transport. In: Handbook of Physiology, Sect 3: The Respiratory System. Vol IV. Gas Exchange. Bethesda, Maryland: American Physiological Society, pp. 147–172, 1987.
[6]Buerk, D. G. An evaluation of Easton's paradigm for the oxyhemoglobin equilibrium curve. *Adv. Exp. Med. Biol.* 180:333–344, 1984.
[7]Buerk, D. G., and E. W. Bridges. A simplified algorithm for computing the variation in oxyhemoglobin saturation with pH, PCO_2, T and DPG. *Chem. Eng. Commun.* 47:113–124, 1986.
[8]Easton, D. M. Oxyhemoglobin dissociation curve as expo-exponential paradigm of asymmetric sigmoid function. *J. Theor. Biol.* 76:335–349, 1979.
[9]Ellis, R. K. Letter to the editor: determination of P_{O_2} from saturation. *J. Appl. Physiol.* 67:902, 1989.
[10]Forster, R. E., H. P. Constantine, M. R. Craw, H. H. Rotman, and R. A. Klocke. Reaction of CO_2 with human hemoglobin solution. *J. Biol. Chem.* 243:3317–3326, 1968.
[11]Forster, R. E. Rate of reaction of CO_2 with human hemoglobin. In: CO_2: Chemical, Biochemical, and Physiological Aspects, edited by R. E. Forster, J. T. Edsall, A. B. Otis, and F. J. W. Roughton. Washington, D.C.: Scientific and Technical Information Division, Office of Technology Utilization, NASA, 1969, pp. 55–59.
[12]Hedley-Whyte, J., and M. B. Laver. O_2 solubility in blood and temperature correction factors for PO_2. *J. Appl. Physiol.* 19:901–906, 1964.
[13]Hill, A. V. The possible effects of the aggregation of the molecules of haemoglobin on its dissociation curves. *J. Physiol.* 40:iv–vii, 1910.
[14]Hill, E. P., G. G. Power, and L. D. Longo. Kinetics of O_2 and CO_2 exchange. In: Bioengineering Aspects of the Lung, edited by J. B. West. New York: Marcel Dekker, 1977, pp. 459–514.
[15]Hill, E. P., G. G. Power, and L. D. Longo. A mathematical model of carbon dioxide transfer in the placenta and its interaction with oxygen. *Am. J. Physiol. Cell Physiol.* 224:283–299, 1973.
[16]Hill, E. P., G. P. Power, and L. D. Longo. Mathematical simulation of pulmonary O_2 and CO_2 exchange. *Am. J. Physiol. Cell Physiol.* 224:904–917, 1973.

[17]Huang, N. S., and J. D. Hellums. A theoretical model for gas transport and acid/base regulation by blood flowing in microvessels. *Microvasc. Res.* 48:364–388, 1994.

[18]Kelman, G. R. Digital computer subroutine for the conversion of oxygen tension into saturation. *J. Appl. Physiol.* 21:1375–1376, 1966.

[19]Kelman, G. R. Calculation of certain indices of cardiopulmonary function using a digital computer. *Respir. Physiol.* 1:335–343, 1966.

[20]Kelman, G. R. Computer program for the production of O_2–CO_2 diagrams. *Respir. Physiol.* 4:260–269, 1968.

[21]Kelman, G. R. Digital computer procedure for the conversion of P_{CO_2} into blood CO_2 content. *Respir. Physiol.*, 3:111–115, 1967.

[22]Klocke RA. Carbon dioxide transport. In: Handbook of Physiology, Sect. 3: The Respiratory System. Vol IV. Gas Exchange. Bethesda, Maryland: American Physiological Society, 1987, pp. 173–197.

[23]Li, Z., T. Yipintsoi, and J. B. Bassingthwaighte. Nonlinear model for capillary-tissue oxygen transport and metabolism. *Ann. Biomed. Eng.* 25:604–619, 1997.

[24]Margaria, R. A mathematical treatment of the blood dissociation curve for oxygen. *Clin. Chem.* 9:745–791, 1963.

[25]Margaria, R., G. Torelli, and A. Pini. A possible mathematical definition of the O_2 dissociation curve from blood or Hb solution. *Exp. Med. Surg.* 21:127–142, 1963.

[26]O'Riordan, J. F., T. K. Goldstick, L. N. Vida, G. R. Honig, and J. T. Ernest. Modelling whole blood oxygen equilibirum: comparison of nine different models fitted to normal human data. *Adv. Exp. Med. Biol.* 191:505–522, 1985.

[27]Popel, A. S. Theory of oxygen transport to tissue. *Crit. Rev. Biomed. Eng.* 17:257–321, 1989.

[28]Roughton, F. J. W., E. C. Deland, J. C. Kernohan, and J. W. Severinghaus. Some recent studies of the oxyhemoglobin dissociation curve of human blood under physiological conditions and the fitting of the Adair equation to the standard curve. In: Oxygen Affinity of Hemoglobin and Red Cell Acid Base Status. Proceedings of the Alfred Benzon Symposium IV Held at the Premises of the Royal Danish Academy of Sciences and Letters, Copenhagen 17–22 May, 1971, edited by M. Rørth and P. Astrup. Copenhagen: Munksgaard, 1972, pp. 73–81.

[29]Roughton, F. J. W. Transport of oxygen and carbon dioxide. In: Handbook of Physiology, Section 3: Respiration. Volume I. Washington, D.C.: American Physiological Society, 1964, pp. 767–825.

[30]Roughton, F. J. W., and J. W. Severinghaus. Accurate determination of O_2 dissociation curve of human blood above 98.7% saturation with data on O_2 solubility in unmodified human blood from 0° to 37° C. *J. Appl. Physiol.* 35:861–869, 1973.

[31]Salathe, E. P., R. Fayad, and S. W. Schaffer. Mathematical analysis of carbon dioxide transfer by blood. *Math. Biosci.* 57:109–153, 1981.

[32]Severinghaus, J. W. Blood gas calculator. *J. Appl. Physiol.* 21:1108–1116, 1966.

[33]Severinghaus, J. W. Simple, accurate equations for human blood O_2 dissociation computations. *J. Appl. Physiol.: Respirat. Environ. Exercise Physiol.* 46:599–602, 1979.

[34]Severinghaus, J. W. Letter to the editor: RE determination of PO_2 from saturation. *J. Appl. Physiol.* 67:902, 1989.

[35]Severinghaus, J. W., M. Stupfel, and A. F. Bradley. Variations of serum carbonic acid pK′ with pH and temperature. *J. Appl. Physiol.* 9:197–200, 1956.

[36]Sharan, M., and M. P. Singh. Equivalence between one step kinetics and Hill's equation. *J. Biomed. Eng.* 6:297–301, 1984.

[37]Siggaard-Andersen, O., P. D. Wimberley, I. Göthgen, and M. Siggard-Andersen. A mathematical model of the hemoglobin-oxygen dissociation curve of human blood and of the oxygen partial pressure as a function of temperature. *Clin. Chem.* 30:1646–1651, 1984.

[38]Singh, M. P., M. Sharan, and A. Aminataei. Development of mathematical formulae for O_2 and CO_2 dissociation curves in the blood. *IMA J. Math. Appl. Med. Biol.* 6:25–46, 1989.

[39]Winslow, R. M., M. Samaja, N. J. Winslow, L. Rossi-Bernardi, and R. I. Shrager. Simulation of continuous blood O_2 equilibrium over physiological pH, DPG, and P_{CO_2} range. *J. Appl. Physiol.: Respirat. Environ. Exercise Physiol.* 54:524–529, 1983.

[40]Winslow, R. M., M.-L. Swenberg, R. L. Berger, R. I. Shrager, M. Luzzana, M. Samaja, and L. Rossi-Bernardi. Oxygen equilibrium curve of normal human blood and its evaluation by Adair's equation. *J. Biol. Chem.* 252:2331–2337, 1977.